
Provably Safe Neural Network Controllers via Differential Dynamic Logic

Samuel Teuber¹ Stefan Mitsch² André Platzer^{1,3}

¹ Karlsruhe Institute of Technology ² DePaul University ³ Carnegie Mellon University
teuber@kit.edu smitsch@depaul.edu platzer@kit.edu

Abstract

While neural networks (NNs) have a large potential as autonomous controllers for Cyber-Physical Systems, verifying the safety of *neural network based control systems (NNCSs)* poses significant challenges for the practical use of NNs—especially when safety is needed for *unbounded time horizons*. One reason for this is the intractability of analyzing NNs, ODEs and hybrid systems. To this end, we introduce VerSAILLE (Verifiably Safe AI via Logically Linked Envelopes): The first general approach that allows reusing control theory literature for NNCS verification. By joining forces, we can exploit the efficiency of NN verification tools while retaining the rigor of differential dynamic logic ($d\mathcal{L}$). Based on a provably safe control envelope in $d\mathcal{L}$, we derive a specification for the NN which is proven with NN verification tools. We show that a proof of the NN’s adherence to the specification is then *mirrored* by a $d\mathcal{L}$ proof on the infinite-time safety of the NNCS.

The NN verification properties resulting from hybrid systems typically contain *nonlinear arithmetic* over formulas with *arbitrary logical structure* while efficient NN verification tools merely support linear constraints. To overcome this divide, we present Mosaic: An efficient, *sound and complete* verification approach for polynomial real arithmetic properties on piece-wise linear NNs. Mosaic partitions complex NN verification queries into simple queries and lifts off-the-shelf linear constraint tools to the nonlinear setting in a completeness-preserving manner by combining approximation with exact reasoning for counterexample regions. In our evaluation we demonstrate the versatility of VerSAILLE and Mosaic: We prove infinite-time safety on the classical Vertical Airborne Collision Avoidance NNCS verification benchmark for some scenarios while (exhaustively) enumerating counterexample regions in unsafe scenarios. We also show that our approach significantly outperforms the State-of-the-Art tools in closed-loop NNV.

1 Introduction

For controllers of Cyber-Physical Systems (CPSs), the use of neural networks (NNs) is both a blessing and a curse. On the one hand, using NNs allows the development of goal-oriented controllers that optimize soft requirements such as passenger comfort, frequency of collision warnings or energy efficiency. On the other hand, guaranteeing that *all* control decisions chosen by an NN are safe is very difficult due to the complex feedback loop between the subsymbolic reasoning of an NN and the intricate dynamics often encountered in physical systems. How can this curse be alleviated? Neural Network Verification (NNV) techniques all have tried one of three strategies: Open-loop NNV entirely omits the analysis of the physical system and only analyzes input-output properties of the NN [11, 21, 41, 42, 56, 57, 90, 93–95]. Open-loop analyses alone cannot justify the safety of an NNCS, because they ignore its physical, feedback-loop dynamics. Closed-loop NNV performs a time-bounded analysis of the feedback loop between the NN and its physical environment [5, 17, 32, 35, 45–47, 82, 85, 88, 89, 92].

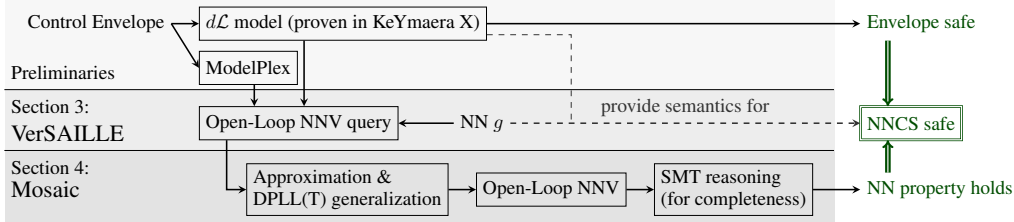


Figure 1: VerSAILLE reflects a proof of a control envelope in an NN to verify infinite-time safety of an NNCS from mere open-loop NNV properties. Mosaic *completely* lifts off-the-shelf open-loop NNV tools to polynomial arithmetic by combining approximation with judicious SMT reasoning.

Unfortunately, a safety guarantee that comes with a time-bound (measured in seconds rather than minutes or hours) is often insufficient when it comes to deploying safety-critical NNCSs in the real world. For example, the safety of an adaptive cruise control system must be independent of the trip length. Finally, another line of work explored techniques for learning and then verifying *approximations of* barrier certificates for infinite-time guarantees [3,8,23,24,29,62]. For *continuous-time*, verification has not been scaled beyond simple linear control functions [23, Appendix] as it requires open-loop NNV w.r.t. nonlinear specifications, which is a notoriously neglected topic [28,29]. Unlike our approach based on differential dynamic logic ($d\mathcal{L}$) [71,75], these techniques also require analytical solutions for the differential equations. Notably, these techniques omit the opportunity to *reuse* control-theory literature where *exact* safe/invariant regions are well understood (e.g. for airborne collision avoidance [48]). How to reuse such knowledge for NNs is a non-trivial matter. While interactive reasoning with $d\mathcal{L}$ is an excellent tool for abstract, nondeterministic control envelopes, the *subsymbolic* reasoning of an NN is entirely beyond its intended purpose. Conversely, neither open/closed-loop NNV tools nor barrier certificate techniques alone are suitable for *exact, infinite-time* control-theory reasoning. Therefore, we propose to combine $d\mathcal{L}$ with open-loop NNV. By combining their strengths, we prove infinite-time safety guarantees for NNCSs that are not provable through either analysis alone.

Overview. This paper alleviates the curse of NNCS safety. As shown in Figure 1, our work integrates the deductive approach of $d\mathcal{L}$ with techniques for open-loop NNV. To apply our approach, we assume that an abstract, nondeterministic control envelope has already been verified in $d\mathcal{L}$ (via KeYmaera X [36] or from the literature). Based on the $d\mathcal{L}$ safety result, VerSAILLE (**V**erifiably **S**afe **A**I via **L**ogically **L**inked **E**nvelopes; Section 3) derives a verification query for open-loop NNV by instrumenting ModelPlex [66]. By reflecting the NN through a *mirror program* in $d\mathcal{L}$, we can then reason about an NNCS in- and outside the $d\mathcal{L}$ calculus simultaneously. The verification of an open-loop NNV query generated by VerSAILLE yields a $d\mathcal{L}$ proof that the NNCS refines a safe control envelope—implying that the infinite-time safety guarantee carries over to the NNCS. Due to the inherent nonlinearities of hybrid systems, the generated open-loop NNV queries often contain polynomial arithmetic and the formulas have arbitrary logical structure. Hence for such queries, we also introduce Mosaic—an efficient, *sound and complete* framework for open-loop NNV tool. The approach *lifts* complete off-the-shelf open-loop NNV tools for linear constraints to *polynomial* constraints with *arbitrary* logical structure by combining approximation and a generalization of DPLL(T) [38] while retaining completeness by generalizing counterexamples into locally affine regions (Section 4). In summary, VerSAILLE provides rigorous semantics and a formal proof of infinite-time safety, while Mosaic makes our approach practically applicable to real-world systems (see also Section 5).

Contribution. Our contribution has three parts. While our implementation (N^3V) supports NNs most commonly analyzed by open-loop NNV (ReLU NNs), our theoretical contribution (VerSAILLE) reaches far beyond this and lays the foundations for analyzing a wide range of NNCS architectures:

- We present VerSAILLE, the formal foundation that, for the first time, enables a *sound proof of infinite-time safety for a concrete NNCS* by reusing safety proofs from control-theory literature (in the form of $d\mathcal{L}$ models). VerSAILLE supports a large class of feed-forward NNs (any NN with piece-wise Noetherian activation functions; see Section 2).
- We introduce Mosaic, an efficient, *sound and complete* technique for verifying properties in *polynomial* real arithmetic with *arbitrary* logical structure on piece-wise linear NNs. Mosaic *lifts* off-the-shelf complete open-loop NNV tools for linear constraints to polynomial

constraints while retaining completeness. Thus, Mosaic is a future-proof vehicle, that allows upgrading sound and complete linear-constraint open-loop NNV tools into sound and complete polynomial constraint tools. The procedure can exhaustively characterize unsafe state space regions which is useful for retraining or the generation of fallback controllers.

- We implement Mosaic for ReLU NNs in the tool N³V and demonstrate our approach on three case studies from adaptive cruise control, airborne collision avoidance ACAS X and steering under uncertainty. We show that, unlike N³V, State-of-the-Art closed-loop NNV tools cannot provide infinite-time guarantees due to approximation errors.

Running Example. The common NNCS safety benchmark of Adaptive Cruise Control [20, 37, 49] will serve as running example to demonstrate the introduced concepts. Consider an ego-car following a front-car on a 1-D lane as shown in Figure 2. The front-car drives with constant velocity v_{const} while the ego-car (at position p_{rel} behind the front-car) approaches with arbitrary initial (relative) velocity v_{rel} which is adjusted through the ego-car’s acceleration a_{rel} . The primary objective is to ensure the ego-car never crashes into the front car (i.e. $p_{rel} > 0$), however there may be secondary objectives (e.g. energy efficiency) which are learned by an NNCS. We demonstrate how a nondeterministic, high-level acceleration strategy (i.e. a safe envelope) can be modeled and verified in $d\mathcal{L}$ (Section 2), how VerSAILLE derives NN properties (Section 3) and how such polynomial properties can be checked on a given NN (Section 4). No techniques are specific to the running example, but all are applicable to a wide range of NNCSs—as demonstrated by our evaluation (Section 5).

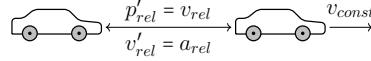


Figure 2: Adaptive Cruise Control: The front-car (right) drives with constant v_{const} . The ego-car approaches with relative velocity v_{rel} (controlled via a_{rel}) from p_{rel} .

2 Background

We review $d\mathcal{L}$, NNs and NN verification. $\text{FOL}_{\mathbb{R}}$ (resp. $\text{FOL}_{\mathbb{L}\mathbb{R}}$) is the set of polynomial (resp. linear) real arithmetic first-order logic formulas. $\text{FOL}_{\mathbb{N}\mathbb{R}}$ extends $\text{FOL}_{\mathbb{R}}$ with *Noetherian functions* [75] h_1, \dots, h_r . A *Noetherian chain* is a sequence of real analytic functions h_1, \dots, h_q s.t. all partial derivatives of all h_j can be written as a polynomial $\frac{\partial h_j(y)}{\partial y_i}(y) = p_{ij}(y, h_1(y), \dots, h_q(y))$. *Noetherian functions* are representable as a polynomial over functions in a Noetherian chain. Most activation functions used in NNs are Noetherian (see overview in Appendix A.2) For a formula ζ , its atoms are denoted as $\text{Atom}(\zeta)$ while its variables are $\text{V}(\zeta)$.

Program	Semantics
$x := e$	Assign term e to x
$x := *$	Nondet. assign to x
$?Q$	Test of formula Q
$x' = t \& Q$	Evolve x along the diff. equation within Q
$\alpha \cup \beta$	Nondet. choice
$\alpha; \beta$	Sequential composition
$(\alpha)^*$	Nondet. loop

Table 1: Program primitives of $d\mathcal{L}$

2.1 Differential Dynamic Logic

Differential dynamic logic ($d\mathcal{L}$) [71–73, 75] is a first-order multi-modal logic in which the modality is parameterized with a *hybrid program* describing a (discrete or continuous) state transition (see also Appendix A). Thus, $d\mathcal{L}$ formulas are evaluated in a state ν (if ν satisfies a formula ψ we denote this as $\nu \models \psi$). Hybrid Programs are constructed from the primitives in Table 1 and are first-class citizens of the logic (see example below). $d\mathcal{L}$ is tailored to the analysis of (time discrete and time continuous) hybrid systems and supports the analysis of differential equations. Through its invariance reasoning capabilities, $d\mathcal{L}$ allows us to prove the infinite-time safety of control-envelopes w.r.t. a system’s dynamics—even for cases where the dynamics’ differential equations have no analytical solution. There is a large body of research on the verification of real-world control envelopes using $d\mathcal{L}$ (e.g. ACAS X [48]). In $d\mathcal{L}$, the formula $[\alpha] \psi$ expresses that ψ is always satisfied after the execution of α and $\langle \alpha \rangle \psi$ that there exists a state satisfying ψ after the execution of α . $d\mathcal{L}$ comes with a sound and relatively complete proof calculus [71, 73, 75] and an interactive theorem prover KeYmaera X [36].

Running Example. We model our running example as a hybrid program in $d\mathcal{L}$ with differential equations describing the evolution of $p_{rel}, v_{rel}, a_{rel}$ along with a *control envelope*, i.e. an abstract

acceleration strategy, α_{ctrl} that runs at least every T seconds while the overall system may run for arbitrarily many iterations (modeled by a nondeterministic loop). Given suitable initial conditions (accInit), our objective is to prove the absence of collisions ($p_{\text{rel}} > 0$). This can be achieved by proving Formula (1) where the place-holder α_{ctrl} determines the relative acceleration $-B \leq a_{\text{rel}} \leq A$ (A and $-B$ are resp. maximal acceleration/braking).

$$\underbrace{\text{accInit}}_{\text{initial conditions}} \rightarrow \left[\left(\underbrace{\alpha_{\text{ctrl}}}_{\text{controller}} ; c := 0 ; \underbrace{(p'_{\text{rel}} = v_{\text{rel}}, v'_{\text{rel}} = -a_{\text{rel}}, c' = 1 \ \& \ c \leq T)}_{\text{environment}} \right)^* \right] \underbrace{p_{\text{rel}} > 0}_{\text{safety constraint}} \quad (1)$$

Our control envelope α_{ctrl} allows braking with $-B$ and an acceleration of 0 or another value if the constraint accCtrl_0 or resp. accCtrl_1 is satisfied (the concrete constraints are found in Appendix D):

$$\alpha_{\text{ctrl}} \equiv a_{\text{rel}} := -B \cup (a_{\text{rel}} := 0 ; ? (\text{accCtrl}_0)) \cup (a_{\text{rel}} := * ; ? (-B \leq a_{\text{rel}} \leq A \wedge \text{accCtrl}_1))$$

The envelope is nondeterministic: While always braking with $-B$ would be safe, an NNCS may *learn* to balance braking with secondary objectives (e.g. minimal acceleration or not falling behind). A proof for Formula (1) in KeYmaera X uses the loop invariant accInv (see Appendix D). Automation of $d\mathcal{L}$ proofs as well as control envelope and invariant synthesis is discussed in the literature [55, 73, 75, 86].

ModelPlex. Many CPS safety properties can be formulated through a $d\mathcal{L}$ formula $\phi \rightarrow \left[(\alpha_{\text{ctrl}} ; \alpha_{\text{plant}})^* \right] \psi$ where ϕ describes initial conditions, and ψ describes the safety criterion to be guaranteed when following the control-plant loop. ModelPlex shielding [66] allows the synthesis of correct-by-construction *controller monitor formulas* ζ_c that ensure an implementation’s runtime behavior matches the envelope α_{ctrl} . Interpreting an implementation’s action as a state transition and denoting the old state’s variables as x_i and the new state’s variables as x_i^+ , ζ_c tells us which combinations of x_i and x_i^+ (i.e. which state transitions) are admissible w.r.t. α_{ctrl} (see Definition 4 in Appendix A).

Running Example. We can apply ModelPlex on the proven contract in Formula (1) to synthesize a monitor for α_{ctrl} . For this simple scenario, the resulting controller monitor formula¹ tells us what new acceleration value a_{rel}^+ may be chosen given the current values of $p_{\text{rel}}, v_{\text{rel}}$:

$$\text{accCtrlFml} \equiv a_{\text{rel}}^+ = B \vee (a_{\text{rel}}^+ = 0 \wedge \text{accCtrl}_0^+) \vee (-B \leq a_{\text{rel}}^+ \leq A \wedge \text{accCtrl}_1^+). \quad (2)$$

Here, accCtrl_i^+ is the constraint accCtrl_i with a_{rel} replaced by a_{rel}^+ . Given an action of a concrete controller implementation that changes a_{rel} to a_{rel}^+ , Formula (2) tells us if this action is in accordance with the strategy modeled by α_{ctrl} , i.e. whether we have a proof of safety for the given state transition.

2.2 Neural Network Verification

This work focuses on feed-forward neural networks typically encountered in NNCSs. The behavior of an NN with input dimension $I \in \mathbb{N}$ and output dimension $O \in \mathbb{N}$ can be summarized as a function $g : \mathbb{R}^I \rightarrow \mathbb{R}^O$. The white-box behavior is described by a sequence of $L \in \mathbb{N}$ hidden layers with dimensions $n^{(k)}$ that iteratively transform an input vector $x^{(0)} \in \mathbb{R}^I$ into an output vector $x^{(L)} \in \mathbb{R}^O$. The computation of layer k is given by $x^{(k+1)} = f^{(k)}(W^{(k)}x^{(k)} + b^{(k)})$, i.e. an affine transformation (with $\text{FOL}_{\mathbb{N}\mathbb{R}}$ representable numbers) followed by a nonlinear activation function $f^{(k)}$. We distinguish different classes of NNs. To this end, we decompose the activation functions $f^{(k)}$ as $f^{(k)}(x) = \sum_{i=1}^s \mathbb{1}_{q_i}(x) f_i(x)$ where f_i are functions, q_i are formulas over $n^{(k)}$ variables and $\mathbb{1}_{q_i}(x)$ is 1 iff $q_i(x)$ is true and 0 otherwise. Table 2 summarizes which results are applicable to which NN class. Each class is a subset of the previous class, i.e. our theory (Section 3) is widely applicable while our implementation (Section 5) focuses on the most common NNs. Open-loop NNV tools analyze NNs in order to verify properties on input-output relations. Their common functionality is reflected in the VNNLIB standard [14, 19]. Off-the-shelf tools are limited to linear, normalized queries (Definition 1). To address this challenge, we present a lifting procedure for the verification of generic (i.e. nonlinear and not normalized) open-loop NNV queries over polynomial real arithmetic (Section 4).

Definition 1 (Open-Loop NNV Query). *An open-loop NNV query consists of a formula $p \in \text{FOL}_{\mathbb{R}}$ over free input variables $Z = \{z_1, \dots, z_I\}$ and output variables x_1^+, \dots, x_O^+ . We call p normalized iff p is a conjunction of some input constraints and a disjunctive normal form over mixed/output constraints, i.e. it has the structure $\bigwedge_j p_{1,j}(z_1, \dots, z_I) \wedge \bigvee_{i \geq 2} \bigwedge_j p_{i,j}(z_1, \dots, z_I, x_1^+, \dots, x_O^+)$, where all $p_{i,j}$ are atomic real arithmetic formulas and all $p_{1,j}$ only contain the free variables from Z . We call a query linear iff $p \in \text{FOL}_{\mathbb{L}\mathbb{R}}$ and call it nonlinear otherwise.*

¹The formula furthermore keeps the new $p_{\text{rel}}^+ v_{\text{rel}}^+$ values unchanged ($p_{\text{rel}} = p_{\text{rel}}^+ \wedge v_{\text{rel}} = v_{\text{rel}}^+$), elided.

NN class	All f_i	All q_i in	Applicable	Decidable	Example
piece-wise Noetherian	Noetherian	$\text{FOL}_{\mathbb{N}\mathbb{R}}$	Section 3		Sigmoid
piece-wise Polynomial	Polynomial	$\text{FOL}_{\mathbb{R}}$	Section 3	✓	x^2
piece-wise Linear	Linear	$\text{FOL}_{\mathbb{L}\mathbb{R}}$	Sections 3 and 4	✓	MaxPool
ReLU	$f^{(k)}(x) = \max(0, x)$		Sections 3 to 5	✓	ReLU

Table 2: Applicability of our results on NNCS safety and decidability of the safety verification problem: Each class is a subset of its predecessor in the table.

3 VerSAILLE: Verifiably Safe AI via Logically Linked Envelopes

We introduce VerSAILLE, our approach for the verification of NNCSs via $d\mathcal{L}$ contracts. The key idea of VerSAILLE are *nondeterministic mirrors*, a mechanism that allows us to reflect a given NN g and reason within and outside of $d\mathcal{L}$ simultaneously. This allows us to instrument open-loop NNV techniques to prove an NN specification outside of $d\mathcal{L}$ which *implies* the safety of a corresponding (mirrored) $d\mathcal{L}$ model describing the NNCS. Reconsider the ACC example (Section 1) for which we synthesized a controller monitor formula in Section 2. The remaining open question is the following:

If we replace the control envelope α_{ctrl} by a given piece-wise Noetherian NN g , does the resulting system retain the same safety guarantees?

Summary of VerSAILLE The input for VerSAILLE is a proven $d\mathcal{L}$ contract. Additionally, one may provide an inductive invariant ζ_s to simplify the subsequent state space analysis. Using ModelPlex’s synthesis of ζ_c , VerSAILLE constructs a nonlinear open-loop NNV query. If we verify this query on an NN g , then the NNCS where we *substitute* the control envelope by g retains the same safety guarantee.

Running Example Since one can only provide formal guarantees for something one can describe formally, we first need a semantics for what it means to substitute α_{ctrl} by g . To this end, we formalize a given piece-wise Noetherian NN g as a hybrid program α_g which we call the *nondeterministic mirror* of g (see Definition 16 and Lemma 17). E.g. for ACC, this program must have two free (i.e. read) variables $p_{\text{rel}}, v_{\text{rel}}$ and one bound (i.e. written) variable a_{rel} and must be designed in such a way that it exactly implements the NN g . Showing safety (see question above) is then equivalent to proving the following $d\mathcal{L}$ formula where α_{plant} describes ACC’s physical dynamics:

$$\text{accInit} \rightarrow \left[(\alpha_g; \alpha_{\text{plant}})^* \right] p_{\text{rel}} > 0. \quad (3)$$

Since NNs do not lend themselves well to interactive analysis, an *automatable* mechanism to prove formula (3) *outside* the $d\mathcal{L}$ calculus is desirable. As discussed in Section 2, we can prove the safety ($p_{\text{rel}} > 0$) of α_{ctrl} via $d\mathcal{L}$. Thus, if we can show that all behavior of the nondeterministic mirror α_g is *already* modeled by α_{ctrl} , the safety guarantee carries over from the envelope to α_g . To show this refinement relation [63, 76], we instrument the controller monitor accCtrlFml in Formula (2). We verify that the NN g satisfies the controller monitor formula accCtrlFml (i.e. we show that g ’s input-output relation satisfies Formula (2)). If this is the case, α_g ’s behavior is modeled by our envelope α_{ctrl} . In practice, it is unnecessary that the behavior of α_g is modeled by α_{ctrl} *everywhere* (e.g. we are not interested in states with $p_{\text{rel}} \leq 0$). It suffices to consider all states within the inductive invariant accInv of the envelope’s system (Formula (1)) as those are precisely the states for which the guarantee on α_{ctrl} holds. Thus, we can prove Formula (3) by showing that g satisfies the following specification for all inputs:

$$\text{accInv} \rightarrow \text{accCtrlFml} \quad (4)$$

VerSAILLE also allows to soundly constrain the system to value ranges where the NN has been trained (Lemma 20). Verifying the queries generated by VerSAILLE with a (nonlinear) open-loop NNV tool (Definition 23) then implies safety of the NNCS (full formalism see Appendix C.1):

Theorem 2 (Soundness). *Let g be a piece-wise Noetherian NN. Further, let $C \equiv (\phi \rightarrow [(\alpha_{\text{ctrl}}; \alpha_{\text{plant}})^*] \psi)$ be a valid contract with controller monitor $\zeta_c \in \text{FOL}_{\mathbb{R}}$ and inductive invariant $\zeta_s \in \text{FOL}_{\mathbb{R}}$. If a sound Nonlinear Neural Network Verifier returns *unsat* for the query $p \equiv (\zeta_s \wedge \neg \zeta_c)$ on g then $\phi \rightarrow [(\alpha_g; \alpha_{\text{plant}})^*] \psi$ is valid.*

If g is piece-wise polynomial, Formula (4) is expressible in $\text{FOL}_{\mathbb{R}}$ and therefore its verification decidable (Lemma 24 which is a special case of [76]). In practice, we can be much more efficient

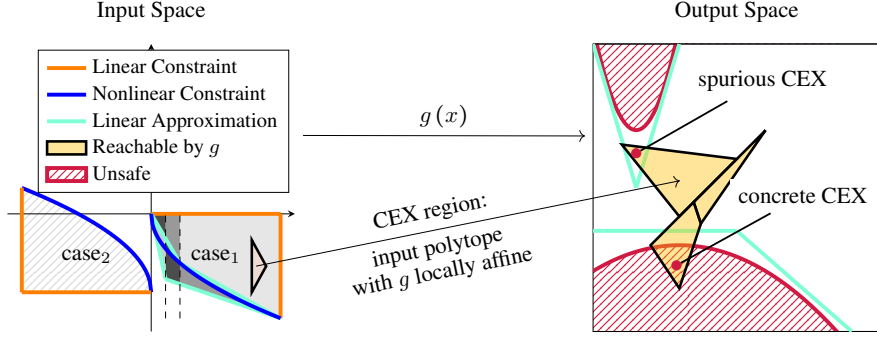


Figure 3: Visualization of the nonlinear verification algorithm Mosaic in Section 4

than naively applying real arithmetic theory solvers by relying on open-loop NNV technologies to check the negated property $\text{accInv} \wedge \neg \text{accCtrlFml}$: If this property is unsatisfiable for a given NN g , then Formula (3) is valid. Off-the-shelf open-loop NNV tools are unable to reason about Formula (4) due to its nonlinearities and the non-normalized formula structure. Thus, our second contribution (Section 4) lifts open-loop NNV tools to the task of verifying nonlinear, non-normalized queries.

4 Mosaic: Nonlinear Open-Loop NN Verification

Since NNCSs usually exhibit nonlinear physical behavior, the verification property $\zeta_s \wedge \neg \zeta_c$ will be nonlinear as well. $\zeta_s \wedge \neg \zeta_c$ is also a formula of arbitrary structure and not a normalized open-loop NNV query (Definition 1). This is evident in the verification query for our running example (see Appendix D) or in Figure 3 where the orange and blue constraints (left) describe two independent nonlinear input regions (case_1 and case_2) and the red regions (right) correspond to the unsafe regions for case_1 . In contrast to this, off-the-shelf open-loop NNV tools (e.g. `nenum` [11] or `Marabou` [57]) only support the verification of linear, normalized open-loop NNV queries on piece-wise linear NNs. Mosaic is a framework that allows us to *lift* off-the-shelf open-loop NNV tools for linear, normalized open-loop NNV queries to polynomial queries of arbitrary logical structure. This approach has the notable advantage that Mosaic’s capabilities grow as open-loop NNV technology evolves while retaining completeness w.r.t. polynomial constraints. An overview of the algorithm is given in Algorithm 1 and Figure 3 which is explained throughout this section with further details in Appendix B.

MOSAIC. To tackle formulas with arbitrary logical structure we could use DNNV [84] which works based on a simple expansion algorithm (i.e. it explodes a given formula into disjunctive normal form). For a formula $P \wedge (Q \vee R)$ this results in two normalized queries $P \wedge Q$ and $P \wedge R$ which are then handed off to the open-loop NNV tool separately. However, if P is the query’s input space constraint (e.g. case_1 in Figure 3) while Q and R describe output space constraints (e.g. the two red regions on the right), this *duplicates* the exploration of P for reachability based open-loop NNV techniques. MOSAIC avoids this inefficiency by generalizing DPLL(T) to construct a *mosaic* over the considered input space where each input region has its own normalized open-loop NNV-query with a disjunction over the output space. In reminiscence of the mosaic analogy, we call the individual queries *azulejos* (see regions in shades of gray in Figure 3). This structure ensures that reachability based open-loop NNV tools do not compute reachable outputs for the same input region multiple times (e.g. for ACAS, naive rewriting could produce up to 39 trillion propositionally feasible conjunctions while MOSAIC only produces 19k queries; see Table 7 in Appendix E.2). MOSAIC also distinguishes nonlinear constraints q_n (must be checked outside open-loop NNV) from linear constraints q_l (can be passed to open-loop NNV) and provably explores no part of the input space twice (see Proposition 10) which improves efficiency in combination with reachability-based open-loop NNV.

LINEARIZE. To verify polynomial specifications via off-the-shelf (linear) open-loop NNV, we need to soundly approximate the query’s nonlinear constraints. In principle, we could perform this approximation for each *azulejo* (see MOSAIC) separately. To this end, consider an atomic polynomial constraint $p(x) \leq 0$ which is part of a query. If there are two *azulejos* with the constraints $p(x) \leq 0$ and $p(x) > 0$, separate approximation would lead to the constraint $\bar{p}(x) \leq 0$ and $\underline{p}(x) > 0$ (with \bar{p}/\underline{p}

Algorithm 1: Verification of nonlinear queries on piece-wise linear NNs: ENUM internally uses off-the-shelf open-loop NNV tools for the verification of linear normalized queries on NNs.

Input: Formula $p \in \text{FOL}_{\mathbb{R}}$, ranges R , piece-wise linear NN g

```

 $p_o \leftarrow \text{LINEARIZE}(p, R)$  ▷ Generate linearized  $p$ 
for all  $(q_l, q_n) \in \text{MOSAIC}(p_o)$  do ▷ Iterate over normalized queries
  for all  $(\iota, \omega) \in \text{ENUM}(g, q_l)$  do ▷ uses GENERALIZE & open-loop NNV
    if  $\text{FILTER}(q_l \wedge q_n, \iota, \omega) = \text{concrete}$  then return unsafe
  return safe ▷ No concrete counterexamples found

```

resp. over/under-approximations of p). This would *duplicate* the exploration of the area in between \bar{p} and \underline{p} and can lead to an exponential blowup for many approximations. Instead, we use a *global* piece-wise approximation via OVERT [85] (aquamarine lines around the dark blue nonlinear constraint on Figure 3) and integrate the approximate constraints into the original query via implications (e.g. we add $\bar{p}(x) \leq 0 \rightarrow p(x) \leq 0$). These additional linear constraints are then automatically enumerated via MOSAIC (see azulejos for case₁ in Figure 3). The linearization happens for input as well as output constraints. When passing the open-loop NNV query to the off-the-shelf tool, we soundly omit the nonlinear constraints, thus only leaving behind linear constraints q_l (aquamarine and orange in Figure 3).

Retaining completeness. Without further efforts, MOSAIC and LINEARIZE together yield a sound algorithm to check nonlinear, not normalized open-loop NNV queries, but not a complete one: A reachability analysis via open-loop NNV for a given azulejo may produce spurious counterexamples that are an artifact of the linearization (see Figure 3) The key insight to achieve completeness is the observation that for piece-wise *linear* NNs any concrete counterexample generated via open-loop NNV corresponds to a *counterexample region* ι (amber polytope on the left of Figure 3) on which the NN reduces to an affine transformation ω (obtained by fixing piece-wise functions to the linear segment of the concrete counterexample, i.e. we fix the value of the $\mathbb{1}$ functions; see also Section 2.2). This insight can be used in two ways: First, we can use it to enumerate all counterexample regions ι (by adjusting the tool’s internal enumeration and/or via the algorithm ENUM; see Appendix B.3). Secondly, for a given counterexample region, we can check whether there exists a concrete counterexample to the nonlinear specification via SMT solving (in Algorithm 1 this is performed by FILTER; see Appendix B.3). By exploiting the affine transformation ω , our SMT encoding for nonlinear constraints has at most I free variables (for I input dimensions of the NN) and is therefore *significantly more tractable* than an encoding of the entire NN in SMT.

Using the components outlined above (for details see Appendix B), we prove the soundness and completeness of Mosaic. Completeness turns out to also be of *practical relevance* as approximation alone would have failed to solve one benchmark discussed in Section 5.

Theorem 3 (Soundness and Completeness). *Let g be a piece-wise linear NN, p be a real arithmetic formula and R variable ranges for all in- and output variables of g . Algorithm 1 returns *unsafe* iff there exists an input $z \in \mathbb{R}^I$ such that $(z, g(z))$ is in the range R and $p(z, g(z))$ is satisfied.*

In Section 5 we build upon nenum [9, 11] which can enumerate all counterexample regions of an NN with N ReLU activations in time $\mathcal{O}(2^N)$, and upon cylindrical algebraic decomposition (CAD; [26]) with complexity $\mathcal{O}(2^{2^V})$ for V variables². Assuming M atomic formulas in the open-loop NNV query and I input dimensions this yields a worst-case runtime of $\mathcal{O}(2^{M+N+2^I})$. This is an exponential improvement over naive $\mathcal{O}(2^{M+2^{N+I}})$ CAD encodings as $N \gg I$. In practice the performance is even better; usually, MOSAIC explores fewer queries, nenum returns less counterexample regions and SMT solving tends to perform very well for small input dimensions I as in NNCS control.

5 Evaluation

We implemented Mosaic for ReLU NNs in a new Julia [15] tool³ called N³V based on the software packages nenum [9, 11], PicoSAT [16, 18] and Z3 [30, 50]. We provide wall-clock times on an

²For simplicity of analysis we fix the complexity’s other variables (e.g. maximal degree).

³See <https://github.com/samysweb/NCubeV>

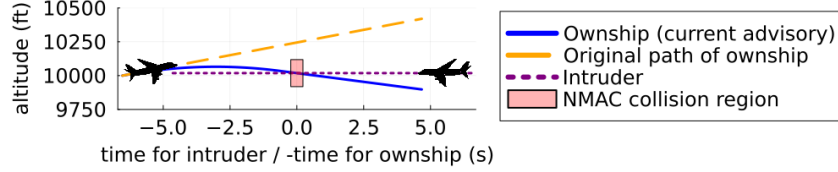


Figure 4: An unsafe advisory by the Airborne Collision Avoidance NN: After a previous advisory to climb at least 1500ft/min, the NN advises to reverse vertical direction (strengthen descent to 1500ft/min). This leads to an NMAC 6 seconds later. More examples are in Appendix G.

AMD Ryzen 7 PRO 5850U CPU (N³V is sequential; nnum uses multithreading). The evaluation presented in this section focuses on vertical airborne collision avoidance (VCAS), with other experiments in Appendix E. Airborne Collision Avoidance Systems try to recognize plane trajectories that might lead to a Near Mid-Air Collision (NMAC) with other aircrafts and advise the pilot to avoid such collisions. NMACs are defined as two planes (ownship and intruder) flying closer than 500 ft horizontally or 100 ft vertically. Currently, the Federal Aviation Administration (FAA) develops a new airborne collision avoidance system called Airborne Collision Avoidance System X (ACAS X) [68]. Prior work by Jeannin et al. [48] showed a nondeterministic, provably safe $d\mathcal{L}$ envelope for airborne collision avoidance. While the original proposal for ACAS X [43, 58] was shown to be unsafe [48], the correctness of a VCAS NN implementation [51, 53] was proven [52] and disproven [54] in varying settings. The proposed NNs contain 6 hidden layers with 45 neurons each and produce one of 9 collision avoidance advisories (*Strengthen Climb to at least 2500 ft/min* (SCL2500) to *Strengthen Descent to at least 2500ft/min* (SDES2500); see Table 9). The objective of the NNs is to ensure safety while minimizing the number of alerts sent to the pilot. We present an *exhaustive* analysis of the VCAS NNCS for level flight intruders. We provide additional experimental results in Appendix E:

- Evaluation of N³V on NNs for our running example (Appendix E.1);
- Appendix E.2 compares N³V to closed-loop NNV (Table 6), DNNV [84] (Table 7), naive SMT solving (Table 8) and Genin et al.’s tailored ACAS approach [40];
- Evaluation on a case-study for Zeppelin steering under uncertainty (Appendix E.3).

Verification Results for VCAS. We reuse the nondeterministic control envelope and loop invariant by Jeannin et al. [48, Thm. 1] to analyze safety for intruders in level flight (i.e. intruder vertical velocity is 0). For the same reasons as prior work [48], we ignore Clear-of-Conflict advisories. The open-loop NNV queries obtained via VerSAILLE had up to 112 distinct atoms and trees up to depth 9. To determine the maximal output neuron, open-loop NNV queries initially contain atoms sorting the NN’s outputs x_1, \dots, x_n (e.g., $x_1 \leq x_2$). To avoid enumerating all permutations (blowing up query size), we perform symmetry elimination by introducing an atomic predicate encoding that some output i is maximal. We analyzed the *full range* of possible NN inputs for intruders in level flight (relative height $|h| \leq 8000$ ft, ownship velocity $|v| \leq 100$ ft/s and time to NMAC $6s \leq \tau \leq 40s$). Our results are in Table 3: **safe** implies that the NN’s advisories (other than Clear-of-Conflict) in this scenario *never* lead to a collision when starting within the invariant. The safety for DNC was only verifiable through SMT filtering (approximation yielded spurious counterexamples). This *underscores the importance of Mosaic’s completeness* and implies that [54] is insufficient to prove safety. A non-exhaustive analysis for non-level flight yielded counterexamples even for DNC/DND (see Appendix G). For unsafe level flight scenarios, we exhaustively characterize unsafe regions going beyond (non-exhaustive) point-wise characterizations via manual approximation [54]. Figure 4 shows a concrete avoidable NMAC (more examples are in Appendix G).

Prev. Adv.	Status	Time	CE regions	First CE
DNC	safe	0.35 h	—	—
DND	safe	0.28 h	—	—
DES1500	unsafe	5.45 h	49,428	0.04 h
CL1500	unsafe	5.18 h	34,658	0.08 h
SDES1500	unsafe	4.05 h	5,360	0.97 h
SCL1500	unsafe	4.89 h	11,323	0.36 h
SDES2500	unsafe	3.66 h	5,259	1.39 h
SCL2500	unsafe	4.45 h	7,846	0.53 h

Table 3: Verification of advisories for ACAS NNs for level flight: Previous advisory, analysis time; number of counterex. regions and time to the discovery of the first counterex.

6 Related Work

Most closely related in its use of $d\mathcal{L}$ is Justified Speculative Control [37]. However, we verify the NNCS *a priori* instead of treating the ML model as a black-box and *a posteriori* using RL runtime enforcement techniques [59]. Similar techniques can be used to train models such that they (probabilistically) conform to a shield/monitor [6]. Principled training methodologies w.r.t. shields are beyond the scope of the current paper. An orthogonal direction of research explores learning Neural Barrier/Lyapunov Functions to prove safety properties [28]. Although initially used for “pure” dynamical and hybrid systems (without NNs) [1, 2, 4, 67, 70, 80, 96, 99], the methods have since been extended to NNCS with discrete [8, 24, 62] and continuous [23, 29, 78] time behavior. While the former works can only approximate continuous time behavior, the latter techniques use off-the-shelf SMT solvers (see also Appendix E.2) for certificate verification which severely limits scalability. While some works ignore verification entirely [29, 78], the remaining work only considered *linear single-layer* NNs [23, Appendix] verified with dReal (see SMT comparison in Appendix E.2). Dawson et al. [29] note “scalable verification for learned certificate functions remains an open problem”. Using N^3V as an alternative to SMT for certificate verification is future work. VerSAILLE evades the necessity to *learn* barrier certificates by reusing established control-theory literature. VEHICLE [27] integrates open-loop NNV with Agda. However, VEHICLE only allows importing normalized, linear properties which limits applicability to CPS verification in realistic settings. Open-loop NNV tools [11, 21, 33, 41, 42, 56, 57, 90, 93–95] do not consider the physical environment and thus *cannot* guarantee the safety of an NNCS. Even in cases where such methods allow nonlinear behavior in activation functions, they do not admit the verification of arbitrary polynomial constraints over the input and output space. Most of these methodologies could be integrated into Mosaic’s framework, i.e. we can lift complete off-the-shelf open-loop NNV tools for the verification of polynomial constraints with arbitrary structure. DNNV [84] previously proposed an approach for open-loop NNV query normalization using a simple expansion algorithm. DNNV has the same limitations as all open-loop NNV tools (no NNCS analysis; no nonlinear constraints) and is less efficient than Mosaic w.r.t. NN reachability analysis (see Section 4). Pre-image computation [60, 65, 98] computes input regions producing a fixed NN prediction. For efficiency, our work constrains the input space with invariants and value ranges—this efficiency would be lost by a backwards computation. Unlike [12, 77], Mosaic supports *arbitrary* polynomial constraints and retains completeness. Moreover, the cited works lack ability to handle arbitrary logical structure and represent open-loop NNV techniques unable to analyze NNCSs. Some prior work used techniques for constructing counterexample regions [31, 97] but only for *individual* datapoints—neither to compute exhaustive characterizations nor to regain completeness for incomplete verifiers. Closed-loop NNV tools [5, 17, 32, 35, 45–47, 82, 85, 88, 89, 92] only consider a fixed time horizon and thus cannot guarantee infinite time horizon safety (see Appendix E.2). Unlike [10, 40, 54], our approach is automated and applicable to *any* CPS expressible in $d\mathcal{L}$ (not just ACAS X; see case studies in Appendix E). Other approaches verify simplified control outputs [40]; rely on hand-crafted approximations while lacking exhaustive counterexamples characterizations [54]; or require quantization effectively analyzing a surrogate system [10].

7 Conclusion and Future Work

This work presents VerSAILLE, the first technique exploiting $d\mathcal{L}$ contracts to prove safety of NNCSs with piece-wise Noetherian NNs. VerSAILLE requires open-loop NNV tools capable of verifying non-normalized polynomial properties which do not exist. Thus, with Mosaic we present an efficient, *sound and complete* approach for the verification of such properties on piece-wise linear NNs. We implemented Mosaic for ReLU NNs in the tool N^3V and demonstrate the applicability and scalability of our approach on multiple case studies (Section 5 and Appendix E). The application to NNCSs by Julian et al. [51, 53] shows that our approach scales even to intricate and high-stakes applications such as airborne collision avoidance. Our results underscore the categorical difference of our approach to closed-loop NNV techniques. Overall, we demonstrate an efficient and generally applicable approach that opens the door for developing of goal-oriented *and* infinite-horizon safe NNCSs in the real world.

Future Work. We believe there is potential for engineering and algorithmic improvements that could further improve the performance of N^3V . Mosaic may be of interest even beyond NNCS verification in VerSAILLE. Since, e.g., neural barrier certificate verification also requires nonlinear open-loop NNV, Mosaic may be equally applicable in this context.

Acknowledgements

This work was supported by funding from the pilot program Core-Informatics of the Helmholtz Association (HGF) and funding provided by an Alexander von Humboldt Professorship. Part of this research was carried out while Samuel Teuber was funded by a scholarship from the International Center for Advanced Communication Technologies (interACT) in cooperation with the Baden Wuerttemberg Foundation.

References

- [1] A. Abate, D. Ahmed, A. Edwards, M. Giacobbe, and A. Peruffo. FOSSIL: a software tool for the formal synthesis of Lyapunov functions and barrier certificates using neural networks. In S. Bogomolov and R. M. Jungers, editors, *HSCC '21: 24th ACM International Conference on Hybrid Systems: Computation and Control, Nashville, Tennessee, May 19-21, 2021*, pages 24:1–24:11. ACM, 2021.
- [2] A. Abate, D. Ahmed, M. Giacobbe, and A. Peruffo. Formal synthesis of Lyapunov neural networks. *IEEE Control. Syst. Lett.*, 5(3):773–778, 2021.
- [3] A. Abate, A. Edwards, and M. Giacobbe. Neural abstractions. In S. Koyejo, S. Mohamed, A. Agarwal, D. Belgrave, K. Cho, and A. Oh, editors, *Advances in Neural Information Processing Systems 35: Annual Conference on Neural Information Processing Systems 2022, NeurIPS 2022, New Orleans, LA, USA, November 28 - December 9, 2022*, 2022.
- [4] D. Ahmed, A. Peruffo, and A. Abate. Automated and sound synthesis of Lyapunov functions with SMT solvers. In A. Biere and D. Parker, editors, *Tools and Algorithms for the Construction and Analysis of Systems - 26th International Conference, TACAS 2020, Held as Part of the European Joint Conferences on Theory and Practice of Software, ETAPS 2020, Dublin, Ireland, April 25-30, 2020, Proceedings, Part I*, volume 12078 of *LNCS*, pages 97–114. Springer, 2020.
- [5] M. E. Akintunde, E. Botoeva, P. Kouvaros, and A. Lomuscio. Formal verification of neural agents in non-deterministic environments. *Auton. Agents Multi Agent Syst.*, 36(1):6, 2022.
- [6] M. Alshiekh, R. Bloem, R. Ehlers, B. Könighofer, S. Niekum, and U. Topcu. Safe reinforcement learning via shielding. In S. A. McIlraith and K. Q. Weinberger, editors, *Proceedings of the Thirty-Second AAAI Conference on Artificial Intelligence, AAAI 18, New Orleans, Louisiana, USA, February 2-7, 2018*, pages 2669–2678. AAAI Press, 2018.
- [7] M. Althoff. An introduction to CORA 2015. In G. Frehse and M. Althoff, editors, *ARCH14-15. 1st and 2nd International Workshop on Applied verification for Continuous and Hybrid Systems*, volume 34 of *EPiC Series in Computing*, pages 120–151. EasyChair, 2015.
- [8] E. Bacci, M. Giacobbe, and D. Parker. Verifying reinforcement learning up to infinity. In Z. Zhou, editor, *Proceedings of the Thirtieth International Joint Conference on Artificial Intelligence, IJCAI 2021, Virtual Event / Montreal, Canada, 19-27 August 2021*, pages 2154–2160. ijcai.org, 2021.
- [9] S. Bak. nenum: Verification of ReLU neural networks with optimized abstraction refinement. In A. Dutle, M. M. Moscato, L. Titolo, C. A. Muñoz, and I. Perez, editors, *NASA Formal Methods - 13th International Symposium, NFM 2021, Virtual Event, May 24-28, 2021, Proceedings*, volume 12673 of *LNCS*, pages 19–36. Springer, 2021.
- [10] S. Bak and H. Tran. Neural network compression of ACAS Xu early prototype is unsafe: Closed-loop verification through quantized state backreachability. In J. V. Deshmukh, K. Havelund, and I. Perez, editors, *NASA Formal Methods - 14th International Symposium, NFM 2022, Pasadena, CA, USA, May 24-27, 2022, Proceedings*, volume 13260 of *LNCS*, pages 280–298. Springer, 2022.
- [11] S. Bak, H. Tran, K. Hobbs, and T. T. Johnson. Improved geometric path enumeration for verifying ReLU neural networks. In S. K. Lahiri and C. Wang, editors, *Computer Aided Verification - 32nd International Conference, CAV 2020, Los Angeles, CA, USA, July 21-24, 2020, Proceedings, Part I*, volume 12224 of *LNCS*, pages 66–96. Springer, 2020.
- [12] M. Balunovic, M. Baader, G. Singh, T. Gehr, and M. T. Vechev. Certifying geometric robustness of neural networks. In H. M. Wallach, H. Larochelle, A. Beygelzimer, F. d’Alché-Buc, E. B. Fox, and R. Garnett, editors, *Advances in Neural Information Processing Systems 32: Annual*

- Conference on Neural Information Processing Systems 2019, NeurIPS 2019, December 8-14, 2019, Vancouver, BC, Canada*, pages 15287–15297, 2019.
- [13] H. Barbosa, C. W. Barrett, M. Brain, G. Kremer, H. Lachnitt, M. Mann, A. Mohamed, M. Mohamed, A. Niemetz, A. Nötzli, A. Ozdemir, M. Preiner, A. Reynolds, Y. Sheng, C. Tinelli, and Y. Zohar. cvc5: A versatile and industrial-strength SMT solver. In D. Fisman and G. Rosu, editors, *Tools and Algorithms for the Construction and Analysis of Systems - 28th International Conference, TACAS 2022, Held as Part of the European Joint Conferences on Theory and Practice of Software, ETAPS 2022, Munich, Germany, April 2-7, 2022, Proceedings, Part I*, volume 13243 of *LNCS*, pages 415–442. Springer, 2022.
 - [14] C. Barrett, G. Katz, D. Guidotti, L. Pulina, N. Narodytska, and A. Tacchella. The VNNLIB standard for benchmarks (draft). Technical report, AIMS-LAB, University of Genoa, 2021.
 - [15] J. Bezanson, A. Edelman, S. Karpinski, and V. B. Shah. Julia: A fresh approach to numerical computing. *SIAM Review*, 59(1):65–98, 9 2017.
 - [16] A. Biere. PicoSAT essentials. *J. Satisf. Boolean Model. Comput.*, 4(2-4):75–97, 2008.
 - [17] S. Bogomolov, M. Forets, G. Frehse, K. Potomkin, and C. Schilling. JuliaReach: a toolbox for set-based reachability. In N. Ozay and P. Prabhakar, editors, *Proceedings of the 22nd ACM International Conference on Hybrid Systems: Computation and Control, HSCC 2019, Montreal, QC, Canada, April 16-18, 2019*, pages 39–44. ACM, 2019.
 - [18] J. Bolewski, C. Lucibello, and M. Bouton. PicoSAT.jl. GitHub, 2024.
 - [19] C. Brix, M. N. Müller, S. Bak, T. T. Johnson, and C. Liu. First three years of the international verification of neural networks competition (VNN-COMP). *Int. J. Softw. Tools Technol. Transf.*, 25(3):329–339, 2023.
 - [20] M. Brosowsky, F. Keck, J. Ketterer, S. Isele, D. Slieter, and M. Zöllner. Safe deep reinforcement learning for adaptive cruise control by imposing state-specific safe sets. In *2021 IEEE Intelligent Vehicles Symposium (IV)*, pages 488–495, 2021.
 - [21] R. Bunel, J. Lu, I. Turkaslan, P. H. S. Torr, P. Kohli, and M. P. Kumar. Branch and bound for piecewise linear neural network verification. *J. Mach. Learn. Res.*, 21:42:1–42:39, 2020.
 - [22] S. Cai, B. Li, and X. Zhang. Local search for SMT on linear integer arithmetic. In S. Shoham and Y. Vizel, editors, *Computer Aided Verification - 34th International Conference, CAV 2022, Haifa, Israel, August 7-10, 2022, Proceedings, Part II*, volume 13372 of *LNCS*, pages 227–248. Springer, 2022.
 - [23] Y. Chang, N. Roohi, and S. Gao. Neural Lyapunov control. In H. M. Wallach, H. Larochelle, A. Beygelzimer, F. d’Alché-Buc, E. B. Fox, and R. Garnett, editors, *Advances in Neural Information Processing Systems 32: Annual Conference on Neural Information Processing Systems 2019, NeurIPS 2019, December 8-14, 2019, Vancouver, BC, Canada*, pages 3240–3249, 2019.
 - [24] S. Chen, M. Fazlyab, M. Morari, G. J. Pappas, and V. M. Preciado. Learning Lyapunov functions for hybrid systems. In *55th Annual Conference on Information Sciences and Systems, CISS 2021, Baltimore, MD, USA, March 24-26, 2021*, page 1. IEEE, 2021.
 - [25] A. Cimatti, A. Griggio, B. J. Schaafsma, and R. Sebastiani. The mathsat5 SMT solver. In N. Piterman and S. A. Smolka, editors, *Tools and Algorithms for the Construction and Analysis of Systems - 19th International Conference, TACAS 2013, Held as Part of the European Joint Conferences on Theory and Practice of Software, ETAPS 2013, Rome, Italy, March 16-24, 2013. Proceedings*, volume 7795 of *LNCS*, pages 93–107. Springer, 2013.
 - [26] G. E. Collins. Quantifier elimination for real closed fields by cylindrical algebraic decomposition-preliminary report. *SIGSAM Bull.*, 8(3):80–90, 1974.
 - [27] M. L. Daggitt, W. Kokke, R. Atkey, L. Arnaboldi, and E. Komendantskaya. Vehicle: Interfacing neural network verifiers with interactive theorem provers. *CoRR*, abs/2202.05207, 2022.
 - [28] C. Dawson, S. Gao, and C. Fan. Safe control with learned certificates: A survey of neural Lyapunov, barrier, and contraction methods for robotics and control. *IEEE Trans. Robotics*, 39(3):1749–1767, 2023.
 - [29] C. Dawson, Z. Qin, S. Gao, and C. Fan. Safe nonlinear control using robust neural Lyapunov-barrier functions. In A. Faust, D. Hsu, and G. Neumann, editors, *Conference on Robot Learning*,

- 8-11 November 2021, London, UK, volume 164 of *Proceedings of Machine Learning Research*, pages 1724–1735. PMLR, 2021.
- [30] L. M. de Moura and N. S. Bjørner. Z3: an efficient SMT solver. In C. R. Ramakrishnan and J. Rehof, editors, *Tools and Algorithms for the Construction and Analysis of Systems, 14th International Conference, TACAS 2008, Held as Part of the Joint European Conferences on Theory and Practice of Software, ETAPS 2008, Budapest, Hungary, March 29-April 6, 2008. Proceedings*, volume 4963 of *LNCS*, pages 337–340. Springer, 2008.
- [31] D. I. Dimitrov, G. Singh, T. Gehr, and M. T. Vechev. Provably robust adversarial examples. In *The Tenth International Conference on Learning Representations, ICLR 2022, Virtual Event, April 25-29, 2022*. OpenReview.net, 2022.
- [32] S. Dutta, X. Chen, and S. Sankaranarayanan. Reachability analysis for neural feedback systems using regressive polynomial rule inference. In N. Ozay and P. Prabhakar, editors, *Proceedings of the 22nd ACM International Conference on Hybrid Systems: Computation and Control, HSCC 2019, Montreal, QC, Canada, April 16-18, 2019*, pages 157–168. ACM, 2019.
- [33] Y. Y. Elboher, J. Gottschlich, and G. Katz. An abstraction-based framework for neural network verification. In S. K. Lahiri and C. Wang, editors, *Computer Aided Verification - 32nd International Conference, CAV 2020, Los Angeles, CA, USA, July 21-24, 2020, Proceedings, Part I*, volume 12224 of *LNCS*, pages 43–65. Springer, 2020.
- [34] C. Eleftheriadis, N. Kekatos, P. Katsaros, and S. Tripakis. On neural network equivalence checking using SMT solvers. In S. Bogomolov and D. Parker, editors, *Formal Modeling and Analysis of Timed Systems - 20th International Conference, FORMATS 2022, Warsaw, Poland, September 13-15, 2022, Proceedings*, volume 13465 of *LNCS*, pages 237–257. Springer, 2022.
- [35] J. Fan, C. Huang, X. Chen, W. Li, and Q. Zhu. ReachNN*: A tool for reachability analysis of neural-network controlled systems. In D. V. Hung and O. Sokolsky, editors, *Automated Technology for Verification and Analysis - 18th International Symposium, ATVA 2020, Hanoi, Vietnam, October 19-23, 2020, Proceedings*, volume 12302 of *LNCS*, pages 537–542. Springer, 2020.
- [36] N. Fulton, S. Mitsch, J. Quesel, M. Völpl, and A. Platzer. KeYmaera X: an axiomatic tactical theorem prover for hybrid systems. In A. P. Felty and A. Middeldorp, editors, *Automated Deduction - CADE-25 - 25th International Conference on Automated Deduction, Berlin, Germany, August 1-7, 2015, Proceedings*, volume 9195 of *LNCS*, pages 527–538. Springer, 2015.
- [37] N. Fulton and A. Platzer. Safe reinforcement learning via formal methods: Toward safe control through proof and learning. In S. A. McIlraith and K. Q. Weinberger, editors, *Proceedings of the Thirty-Second AAAI Conference on Artificial Intelligence, (AAAI-18), New Orleans, Louisiana, USA, February 2-7, 2018*, pages 6485–6492. AAAI Press, 2018.
- [38] H. Ganzinger, G. Hagen, R. Nieuwenhuis, A. Oliveras, and C. Tinelli. DPLL(T): fast decision procedures. In R. Alur and D. A. Peled, editors, *Computer Aided Verification, 16th International Conference, CAV 2004, Boston, MA, USA, July 13-17, 2004, Proceedings*, volume 3114 of *LNCS*, pages 175–188. Springer, 2004.
- [39] S. Gao, S. Kong, and E. M. Clarke. dReal: An SMT solver for nonlinear theories over the reals. In M. P. Bonacina, editor, *Automated Deduction - CADE-24 - 24th International Conference on Automated Deduction, Lake Placid, NY, USA, June 9-14, 2013. Proceedings*, volume 7898 of *LNCS*, pages 208–214. Springer, 2013.
- [40] D. Genin, I. Papusha, J. Brulé, T. Young, G. E. Mullins, Y. Kouskoulas, R. Wu, and A. C. Schmidt. Formal verification of neural network controllers for collision-free flight. In R. Bloem, R. Dimitrova, C. Fan, and N. Sharygina, editors, *Software Verification - 13th International Conference, VSTTE 2021, New Haven, CT, USA, October 18-19, 2021, and 14th International Workshop, NSV 2021, Los Angeles, CA, USA, July 18-19, 2021, Revised Selected Papers*, volume 13124 of *LNCS*, pages 147–164. Springer, 2021.
- [41] P. Henriksen and A. Lomuscio. DEEPSPLIT: an efficient splitting method for neural network verification via indirect effect analysis. In Z. Zhou, editor, *Proceedings of the Thirtieth International Joint Conference on Artificial Intelligence, IJCAI 2021, Virtual Event / Montreal, Canada, 19-27 August 2021*, pages 2549–2555. ijcai.org, 2021.
- [42] P. Henriksen and A. R. Lomuscio. Efficient neural network verification via adaptive refinement and adversarial search. In G. D. Giacomo, A. Catalá, B. Dilkina, M. Milano, S. Barro,

- A. Bugarín, and J. Lang, editors, *ECAI 2020 - 24th European Conference on Artificial Intelligence, 29 August-8 September 2020, Santiago de Compostela, Spain, August 29 - September 8, 2020*, volume 325 of *Frontiers in Artificial Intelligence and Applications*, pages 2513–2520. IOS Press, 2020.
- [43] J. E. Holland, M. J. Kochenderfer, and W. A. Olson. Optimizing the next generation collision avoidance system for safe, suitable, and acceptable operational performance. *Air Traffic Control Quarterly*, 21(3):275–297, 2013.
- [44] C. Huang, J. Fan, X. Chen, W. Li, and Q. Zhu. POLAR: A polynomial arithmetic framework for verifying neural-network controlled systems. In A. Bouajjani, L. Holík, and Z. Wu, editors, *Automated Technology for Verification and Analysis - 20th International Symposium, ATVA 2022, Virtual Event, October 25-28, 2022, Proceedings*, volume 13505 of *LNCS*, pages 414–430. Springer, 2022.
- [45] C. Huang, J. Fan, W. Li, X. Chen, and Q. Zhu. ReachNN: Reachability analysis of neural-network controlled systems. *ACM Trans. Embed. Comput. Syst.*, 18(5s):106:1–106:22, 2019.
- [46] R. Ivanov, T. J. Carpenter, J. Weimer, R. Alur, G. J. Pappas, and I. Lee. Verifying the safety of autonomous systems with neural network controllers. *ACM Trans. Embed. Comput. Syst.*, 20(1):7:1–7:26, 2021.
- [47] R. Ivanov, T. J. Carpenter, J. Weimer, R. Alur, G. J. Pappas, and I. Lee. Verisig 2.0: Verification of neural network controllers using Taylor model preconditioning. In A. Silva and K. R. M. Leino, editors, *Computer Aided Verification - 33rd International Conference, CAV 2021, Virtual Event, July 20-23, 2021, Proceedings, Part I*, volume 12759 of *LNCS*, pages 249–262. Springer, 2021.
- [48] J. Jeannin, K. Ghorbal, Y. Kouskoulas, A. C. Schmidt, R. W. Gardner, S. Mitsch, and A. Platzer. A formally verified hybrid system for safe advisories in the next-generation airborne collision avoidance system. *Int. J. Softw. Tools Technol. Transf.*, 19(6):717–741, 2017.
- [49] T. T. Johnson, D. M. Lopez, L. Benet, M. Forets, S. Guadalupe, C. Schilling, R. Ivanov, T. J. Carpenter, J. Weimer, and I. Lee. ARCH-COMP21 category report: Artificial intelligence and neural network control systems (AINNCS) for continuous and hybrid systems plants. In G. Frehse and M. Althoff, editors, *8th International Workshop on Applied Verification of Continuous and Hybrid Systems (ARCH21), Brussels, Belgium, July 9, 2021*, volume 80 of *EPiC Series in Computing*, pages 90–119. EasyChair, 2021.
- [50] D. Jovanovic and L. de Moura. Solving non-linear arithmetic. *ACM Commun. Comput. Algebra*, 46(3/4):104–105, 2012.
- [51] K. D. Julian. *Safe and efficient aircraft guidance and control using neural networks*. PhD thesis, Stanford University, 2020.
- [52] K. D. Julian and M. J. Kochenderfer. Guaranteeing safety for neural network-based aircraft collision avoidance systems. In *2019 IEEE/AIAA 38th Digital Avionics Systems Conference (DASC)*, pages 1–10, 2019.
- [53] K. D. Julian, J. Lopez, J. S. Brush, M. P. Owen, and M. J. Kochenderfer. Policy compression for aircraft collision avoidance systems. In *2016 IEEE/AIAA 35th Digital Avionics Systems Conference (DASC)*, pages 1–10, 2016.
- [54] K. D. Julian, S. Sharma, J.-B. Jeannin, and M. J. Kochenderfer. Verifying aircraft collision avoidance neural networks through linear approximations of safe regions. In *Verification of Neural Networks (VNN 2019)*, 2019.
- [55] A. Kabra, J. Laurent, S. Mitsch, and A. Platzer. CESAR: Control envelope synthesis via angelic refinements. In B. Finkbeiner and L. Kovács, editors, *TACAS*, volume 14570 of *LNCS*, pages 144–164. Springer, 2024.
- [56] G. Katz, C. W. Barrett, D. L. Dill, K. Julian, and M. J. Kochenderfer. Reluplex: An efficient SMT solver for verifying deep neural networks. In R. Majumdar and V. Kuncak, editors, *Computer Aided Verification - 29th International Conference, CAV 2017, Heidelberg, Germany, July 24-28, 2017, Proceedings, Part I*, volume 10426 of *LNCS*, pages 97–117. Springer, 2017.
- [57] G. Katz, D. A. Huang, D. Ibeling, K. Julian, C. Lazarus, R. Lim, P. Shah, S. Thakoor, H. Wu, A. Zeljic, D. L. Dill, M. J. Kochenderfer, and C. W. Barrett. The Marabou framework for verification and analysis of deep neural networks. In I. Dillig and S. Tasiran, editors, *Computer*

- Aided Verification - 31st International Conference, CAV 2019, New York City, NY, USA, July 15-18, 2019, Proceedings, Part I*, volume 11561 of *LNCS*, pages 443–452. Springer, 2019.
- [58] M. J. Kochenderfer, J. E. Holland, and J. P. Chryssanthacopoulos. Next generation airborne collision avoidance system. *Lincoln Laboratory Journal*, 19(1):17–33, 2012.
- [59] B. Könighofer, R. Bloem, R. Ehlers, and C. Pek. Correct-by-construction runtime enforcement in AI - A survey. In *Principles of Systems Design - Essays Dedicated to Thomas A. Henzinger on the Occasion of His 60th Birthday*, pages 650–663, 2022.
- [60] S. Kotha, C. Brix, J. Z. Kolter, K. Dvijotham, and H. Zhang. Provably bounding neural network preimages. *Advances in Neural Information Processing Systems*, 36, 2024.
- [61] V. Kunc and J. Kléma. Three decades of activations: A comprehensive survey of 400 activation functions for neural networks, 2024.
- [62] M. Lechner, D. Zikelic, K. Chatterjee, and T. A. Henzinger. Infinite time horizon safety of Bayesian neural networks. In M. Ranzato, A. Beygelzimer, Y. N. Dauphin, P. Liang, and J. W. Vaughan, editors, *Advances in Neural Information Processing Systems 34: Annual Conference on Neural Information Processing Systems 2021, NeurIPS 2021, December 6-14, 2021, virtual*, pages 10171–10185, 2021.
- [63] S. M. Loos and A. Platzer. Differential refinement logic. In M. Grohe, E. Koskinen, and N. Shankar, editors, *Proceedings of the 31st Annual ACM/IEEE Symposium on Logic in Computer Science, LICS '16, New York, NY, USA, July 5-8, 2016*, pages 505–514. ACM, 2016.
- [64] D. M. Lopez, M. Althoff, L. Benet, X. Chen, J. Fan, M. Forets, C. Huang, T. T. Johnson, T. Ladner, W. Li, et al. ARCH-COMP22 category report: Artificial intelligence and neural network control systems (AINNCS) for continuous and hybrid systems plants. In *Proceedings of 9th International Workshop on Applied*, volume 90, pages 142–184, 2022.
- [65] K. Matoba and F. Fleuret. Exact preimages of neural network aircraft collision avoidance systems. In *Proceedings of the Machine Learning for Engineering Modeling, Simulation, and Design Workshop at Neural Information Processing Systems*, volume 2020, 2020.
- [66] S. Mitsch and A. Platzer. ModelPlex: verified runtime validation of verified cyber-physical system models. *Formal Methods Syst. Des.*, 49(1-2):33–74, 2016.
- [67] N. Noroozi, P. Karimghaee, F. Safaei, and H. Javadi. Generation of Lyapunov functions by neural networks. In *Proceedings of the World Congress on Engineering*, volume 2008, 2008.
- [68] W. A. Olson. Airborne collision avoidance system X. Technical report, Massachusetts Institute of Technology Lexington Lincoln Lab, 2015.
- [69] I. Papusha, R. Wu, J. Brulé, Y. Kouskoulas, D. Genin, and A. Schmidt. Incorrect by Construction: Fine Tuning Neural Networks for Guaranteed Performance on Finite Sets of Examples. In *3rd Workshop on Formal Methods for ML-Enabled Autonomous Systems (FOMLAS)*, pages 1–12, 2020.
- [70] A. Peruffo, D. Ahmed, and A. Abate. Automated and formal synthesis of neural barrier certificates for dynamical models. In J. F. Groote and K. G. Larsen, editors, *Tools and Algorithms for the Construction and Analysis of Systems - 27th International Conference, TACAS 2021, Held as Part of the European Joint Conferences on Theory and Practice of Software, ETAPS 2021, Luxembourg City, Luxembourg, March 27 - April 1, 2021, Proceedings, Part I*, volume 12651 of *LNCS*, pages 370–388. Springer, 2021.
- [71] A. Platzer. Differential dynamic logic for hybrid systems. *J. Autom. Reason.*, 41(2):143–189, 2008.
- [72] A. Platzer. The complete proof theory of hybrid systems. In *Proceedings of the 27th Annual IEEE Symposium on Logic in Computer Science, LICS 2012, Dubrovnik, Croatia, June 25-28, 2012*, pages 541–550. IEEE Computer Society, 2012.
- [73] A. Platzer. A complete uniform substitution calculus for differential dynamic logic. *J. Autom. Reason.*, 59(2):219–265, 2017.
- [74] A. Platzer. Differential hybrid games. *ACM Trans. Comput. Log.*, 18(3):19:1–19:44, 2017.
- [75] A. Platzer and Y. K. Tan. Differential equation invariance axiomatization. *J. ACM*, 67(1):6:1–6:66, 2020.
- [76] E. Prebet and A. Platzer. Uniform substitution for differential refinement logic, 2024.

- [77] C. Qin, K. D. Dvijotham, B. O’Donoghue, R. Bunel, R. Stanforth, S. Goyal, J. Uesato, G. Swirszcz, and P. Kohli. Verification of non-linear specifications for neural networks. In *7th International Conference on Learning Representations, ICLR 2019, New Orleans, LA, USA, May 6-9, 2019*, 2019.
- [78] Z. Qin, K. Zhang, Y. Chen, J. Chen, and C. Fan. Learning safe multi-agent control with decentralized neural barrier certificates. In *9th International Conference on Learning Representations, ICLR 2021, Virtual Event, Austria, May 3-7, 2021*. OpenReview.net, 2021.
- [79] A. Raffin, A. Hill, A. Gleave, A. Kanervisto, M. Ernestus, and N. Dormann. Stable-baselines3: Reliable reinforcement learning implementations. *J. Mach. Learn. Res.*, 22:268:1–268:8, 2021.
- [80] S. M. Richards, F. Berkenkamp, and A. Krause. The Lyapunov neural network: Adaptive stability certification for safe learning of dynamical systems. In *2nd Annual Conference on Robot Learning, CoRL 2018, Zürich, Switzerland, 29-31 October 2018, Proceedings*, volume 87 of *Proceedings of Machine Learning Research*, pages 466–476. PMLR, 2018.
- [81] M. Sälzer and M. Lange. Reachability is NP-complete even for the simplest neural networks. In P. C. Bell, P. Totzke, and I. Potapov, editors, *Reachability Problems - 15th International Conference, RP 2021, Liverpool, UK, October 25-27, 2021, Proceedings*, volume 13035 of *LNCS*, pages 149–164. Springer, 2021.
- [82] C. Schilling, M. Forets, and S. Guadalupe. Verification of neural-network control systems by integrating Taylor models and zonotopes. *CoRR*, abs/2112.09197, 2021.
- [83] S. Sharma, S. Roy, M. Soos, and K. S. Meel. Ganak: A scalable probabilistic exact model counter. In *Proceedings of International Joint Conference on Artificial Intelligence (IJCAI)*, 8 2019.
- [84] D. Shriver, S. G. Elbaum, and M. B. Dwyer. DNNV: A framework for deep neural network verification. In A. Silva and K. R. M. Leino, editors, *Computer Aided Verification - 33rd International Conference, CAV 2021, Virtual Event, July 20-23, 2021, Proceedings, Part I*, volume 12759 of *LNCS*, pages 137–150. Springer, 2021.
- [85] C. Sidrane, A. Maleki, A. Irfan, and M. J. Kochenderfer. OVERT: an algorithm for safety verification of neural network control policies for nonlinear systems. *Journal of Machine Learning Research*, 23(117):1–45, 2022.
- [86] A. Sogokon, S. Mitsch, Y. K. Tan, K. Cordwell, and A. Platzer. Pegasus: Sound continuous invariant generation. *Form. Methods Syst. Des.*, 58(1):5–41, 2022. Special issue for selected papers from FM’19.
- [87] A. Tarski. *A Decision Method for Elementary Algebra and Geometry*. University of California Press, Berkeley and Los Angeles, 1951.
- [88] H. Tran, D. M. Lopez, P. Musau, X. Yang, L. V. Nguyen, W. Xiang, and T. T. Johnson. Star-based reachability analysis of deep neural networks. In M. H. ter Beek, A. McIver, and J. N. Oliveira, editors, *Formal Methods - The Next 30 Years - Third World Congress, FM 2019, Porto, Portugal, October 7-11, 2019, Proceedings*, volume 11800 of *LNCS*, pages 670–686. Springer, 2019.
- [89] H. Tran, X. Yang, D. M. Lopez, P. Musau, L. V. Nguyen, W. Xiang, S. Bak, and T. T. Johnson. NNV: the neural network verification tool for deep neural networks and learning-enabled cyber-physical systems. In S. K. Lahiri and C. Wang, editors, *Computer Aided Verification - 32nd International Conference, CAV 2020, Los Angeles, CA, USA, July 21-24, 2020, Proceedings, Part I*, volume 12224 of *LNCS*, pages 3–17. Springer, 2020.
- [90] S. Wang, H. Zhang, K. Xu, X. Lin, S. Jana, C. Hsieh, and J. Z. Kolter. Beta-crown: Efficient bound propagation with per-neuron split constraints for neural network robustness verification. In M. Ranzato, A. Beygelzimer, Y. N. Dauphin, P. Liang, and J. W. Vaughan, editors, *Advances in Neural Information Processing Systems 34: Annual Conference on Neural Information Processing Systems 2021, NeurIPS 2021, December 6-14, 2021, virtual*, pages 29909–29921, 2021.
- [91] Wolfram Research Inc. Mathematica, Version 14.0. Champaign, IL, 2024.
- [92] W. Xiang, H. Tran, X. Yang, and T. T. Johnson. Reachable set estimation for neural network control systems: A simulation-guided approach. *IEEE Trans. Neural Networks Learn. Syst.*, 32(5):1821–1830, 2021.

- [93] K. Xu, Z. Shi, H. Zhang, Y. Wang, K. Chang, M. Huang, B. Kailkhura, X. Lin, and C. Hsieh. Automatic perturbation analysis for scalable certified robustness and beyond. In H. Larochelle, M. Ranzato, R. Hadsell, M. Balcan, and H. Lin, editors, *Advances in Neural Information Processing Systems 33: Annual Conference on Neural Information Processing Systems 2020, NeurIPS 2020, December 6-12, 2020, virtual*, 2020.
- [94] K. Xu, H. Zhang, S. Wang, Y. Wang, S. Jana, X. Lin, and C. Hsieh. Fast and complete: Enabling complete neural network verification with rapid and massively parallel incomplete verifiers. In *9th International Conference on Learning Representations, ICLR 2021, Virtual Event, Austria, May 3-7, 2021*, 2021.
- [95] H. Zhang, T. Weng, P. Chen, C. Hsieh, and L. Daniel. Efficient neural network robustness certification with general activation functions. In S. Bengio, H. M. Wallach, H. Larochelle, K. Grauman, N. Cesa-Bianchi, and R. Garnett, editors, *Advances in Neural Information Processing Systems 31: Annual Conference on Neural Information Processing Systems 2018, NeurIPS 2018, December 3-8, 2018, Montréal, Canada*, pages 4944–4953, 2018.
- [96] H. Zhang, J. Wu, Y. Vorobeychik, and A. Clark. Exact verification of ReLU neural control barrier functions. In A. Oh, T. Naumann, A. Globerson, K. Saenko, M. Hardt, and S. Levine, editors, *Advances in Neural Information Processing Systems 36: Annual Conference on Neural Information Processing Systems 2023, NeurIPS 2023, New Orleans, LA, USA, December 10-16, 2023*, 2023.
- [97] X. Zhang, A. Solar-Lezama, and R. Singh. Interpreting neural network judgments via minimal, stable, and symbolic corrections. In S. Bengio, H. M. Wallach, H. Larochelle, K. Grauman, N. Cesa-Bianchi, and R. Garnett, editors, *Advances in Neural Information Processing Systems 31: Annual Conference on Neural Information Processing Systems 2018, NeurIPS 2018, December 3-8, 2018, Montréal, Canada*, pages 4879–4890, 2018.
- [98] X. Zhang, B. Wang, and M. Kwiatkowska. Provable preimage under-approximation for neural networks. In B. Finkbeiner and L. Kovács, editors, *Tools and Algorithms for the Construction and Analysis of Systems*, pages 3–23, Cham, 2024. Springer Nature Switzerland.
- [99] Q. Zhao, X. Chen, Y. Zhang, M. Sha, Z. Yang, W. Lin, E. Tang, Q. Chen, and X. Li. Synthesizing ReLU neural networks with two hidden layers as barrier certificates for hybrid systems. In S. Bogomolov and R. M. Jungers, editors, *HSCC '21: 24th ACM International Conference on Hybrid Systems: Computation and Control, Nashville, Tennessee, May 19-21, 2021*, pages 17:1–17:11. ACM, 2021.

A Additional Background

This section provides additional background on Differential Dynamic Logic and the status of various activation functions w.r.t. our classification in Table 2.

A.1 Differential Dynamic Logic

Differential dynamic logic ($d\mathcal{L}$) [71–73, 75] can analyze models of hybrid systems that are described through *hybrid programs*. The syntax of hybrid programs with Noetherian functions is defined by the following grammar, where the term e and formula Q are over real arithmetic with Noetherian functions:

$$\alpha, \beta ::= x := e \mid x := * \mid ?Q \mid x' = f(x) \& Q \mid \alpha \cup \beta \mid \alpha; \beta \mid \alpha^* \quad (5)$$

The semantics of hybrid programs are defined by a transition relation over states in the set \mathcal{S} , each assigning real values to all variables. For example, the assignment state transition relation is defined as $\llbracket x := e \rrbracket = \{(\nu, \omega) \in \mathcal{S}^2 \mid \omega = \nu_x^{(e)}\}$ where $\nu_x^{(e)}$ denotes the state that is equal to ν everywhere except for the value of x , which is modified to $\nu(e)$. The other programs in the same order as in (5) describe nondeterministic assignment of x , test of a predicate Q , continuous evolution along the differential equation within domain Q , nondeterministic choice, sequential composition, and nondeterministic repetition. For a given program α , we distinguish between bound variables $BV(\alpha)$ and free variables $FV(\alpha)$ where bound variables are (potentially) written to, and free variables are read. The formula $\llbracket \alpha \rrbracket \psi$ expresses that ψ is always satisfied after the execution of α and $\langle \alpha \rangle \psi$ that there exists a state satisfying ψ after the execution of α . If a state ν satisfies ψ we denote this as

$\nu \models \psi$. $d\mathcal{L}$ comes with a sound and relatively complete proof calculus [71, 73, 75] as well as the interactive theorem prover KeYmaera X [36].

ModelPlex. As demonstrated in the example, many safety properties for CPSs can be formulated through a $d\mathcal{L}$ formula with a loop in which α_{ctrl} describes the (discrete) software, and α_{plant} describes the (continuous) physical environment:

$$\phi \rightarrow \left[(\alpha_{\text{ctrl}}; \alpha_{\text{plant}})^* \right] \psi. \quad (6)$$

ϕ describes initial conditions, and ψ describes the safety criterion to be guaranteed when following the control-plant loop. To ensure that the behavior of controllers and plants in practice match all assumptions represented in the contract, ModelPlex shielding [66] synthesizes correct-by-construction monitors for CPSs. ModelPlex can also synthesize a correct controller monitor formula ζ_c (Definition 4). The formula ζ_c encodes a relation between two states. If ζ_c is satisfied, then the variable change from x_i to x_i^+ corresponds to behavior modeled by α_{ctrl} , i.e. the change upholds the guarantee from Formula (6). To reason about this state relation, we say that a state tuple (ν, ω) satisfies a formula ζ (denoted as $(\nu, \omega) \models \zeta$) iff $\nu \stackrel{\omega(x_1) \dots \omega(x_n)}{x_1^+ \dots x_n^+} \models \zeta$ (i.e. ν with the new state's value $\omega(x_i)$ as the value of x_i^+ for all i , satisfies ζ).

Definition 4 (Correct Controller Monitor [66]). *A controller monitor formula ζ_c with free variables $x_1, x_1^+, \dots, x_n, x_n^+$ is called correct for the hybrid program controller α_{ctrl} with bound variables x_1, \dots, x_n iff the following $d\mathcal{L}$ formula is valid: $\zeta_c \rightarrow \langle \alpha_{\text{ctrl}} \rangle \bigwedge_{i=1}^n x_i = x_i^+$.*

A.2 Classification of Activation Functions

Table 4 is meant to provide a brief overview on the status of various common activation functions w.r.t. the classes from Table 2. The chosen activation functions are representative examples from the comprehensive survey by Kunc et al. [61]. For piece-wise polynomial and Noetherian functions, any activation function represented by a polynomial over the activation functions presented in Table 4 is resp. piece-wise polynomial or Noetherian. For piece-wise linear functions, any linear combination is resp. piece-wise linear. This table does not claim to be comprehensive—many more activation functions can be classified into one of the categories.

Activation Function	Justification
ReLU NNs	
ReLU	ReLU
piece-wise linear NNs	
LeakyReLU [61, 3.6.2]	Split into < 0 and ≥ 0 .
HardTanh [61, 3.6.18]	Split into 3 regions.
piece-wise polynomial NNs	
Square-based activation functions [61, 3.8]	by definition.
Polynomial universal activation function [61, 3.16]	by definition for integer exponents.
piece-wise Noetherian NNs	
Sigmoid [61, 3.2]	$\sigma'(x) = \sigma(x)(1 - \sigma(x))$
Tanh [61, 3.2]	$\tanh(x) = 2\sigma(2x) - 1$
Arctan [61, 3.2.4]	$\arctan'(x) = 1/(1 + x^2)$
SiLU [61, 3.3]	Polynomial over σ
$\exp(x)$	$\exp'(x) = \exp(x)$
GELU [61, 3.3.1]	In a Noetherian Chain with \exp and the gaussian error function
Approximate GELU [61, 3.3.1]	Polynomial over σ or \tanh
Softmax [61, 3.5] ^a	Polynomial over \exp .

Table 4: Overview on classification of activation functions.

^aThe analysis of softmax can often be avoided by using the observation that its application does not change the order of outcomes, i.e. for classification-like tasks we can use the maximum before Softmax application instead.

B Mosaic

An overview of the algorithm is given in Figure 3: A piece-wise linear NN g is a function which maps from an input space (left) to an output space (right). We consider a part of the input space that is constrained by linear (orange) and nonlinear constraints (blue). As our query is not normalized, it may talk about multiple parts of the input space, e.g. in our case the two sets labeled with case_1 and case_2 . For any such part of the input space, say case_1 , we have a specification about *unsafe* parts of the output space which must not be entered (red dashed areas on the right). For classical open-loop NNV the task is then, given a single input polytope, to compute the set of reachable outputs for g and to check whether there exists an output reaching an unsafe output polytope. In our case the task is more complicated, because the input is not a polytope, but an arbitrary polynomial constraint. Moreover, for each polynomial input constraint (case_1 and case_2 in Figure 3) we may have different nonlinear unsafe output sets. In order to retain soundness, we over- *and* underapproximate nonlinear constraints (see turquoise linear approximations around the blue and red nonlinear constraints in Figure 3). Once all nonlinear queries have approximations, we generate a *mosaic* of the input space where each *azulejo* (i.e. each input region) has its own normalized open-loop NNV-query (polytope over the input; disjunction of polytopes over the output). We must not only split between the two original cases (case_1 and case_2), but also between different segments of the approximating constraints (see the polytopes on the left in four shades of gray). Each normalized query has associated nonlinear constraints that must be satisfied, but cannot be checked via off-the-shelf open-loop NNV tools. Using the normalized, linear open-loop NNV queries we then instrument off-the-shelf tools to check whether any overapproximated unsafe region (turquoise on the right) is reachable. The amber colored regions represent parts of the outputs reachable by g : As can be seen by the two red dots, a reachable point within the overapproximated unsafe region may be a concrete unsafe output, or it may be spuriously unsafe due to the overapproximation. To retain completeness, we need to exhaustively filter spurious counterexamples. This is achieved by *generalizing* the counterexample to a region around the point in which the behavior of g is equivalent to a single affine transformation. Such counterexample regions always exist due to g 's piece-wise linearity. For example, in Figure 3 g affinely maps the input space triangle (left) to the upper output space triangle (in amber on the right). We can then check for concrete counterexamples in this region w.r.t. the affine transformation using an SMT solver. This avoids the need to encode the entire NN in an SMT formula. By excluding explored regions, we can then enumerate all counterexample regions and thus characterize the unsafe input set.

The approach is outlined in Algorithm 1 and proceeds in four steps, all of which will be presented in detail throughout the sections below: First, LINEARIZE generates approximate linearized versions for all nonlinear atoms of p on a bounded domain and enriches the formula with these constraints (p_o). Next, MOSAIC generates a mosaic of p_o 's input space where each *azulejo* (i.e. each input space region) has an associated linear normalized query q_l . Each q_l is paired with an associated disjunctive normal form of nonlinear constraints q_n . The disjunction over all $q_l \wedge q_n$ is equivalent to the input query p_o and the disjunction over all q_l overapproximates LINEARIZE's input p . Each of the linear queries q_l is processed by ENUM which internally uses an off-the-shelf open-loop NNV tool to enumerate all counterexample regions for a given query. Each counterexample region is defined through a polytope in the input space $\iota \subset \mathbb{R}^I$ and an affine mapping to the output space $\omega : \mathbb{R}^I \rightarrow \mathbb{R}^O$ that summarizes the NN's local behavior in ι . The procedure FILTER then checks whether a counterexample region is spurious using an SMT solver. This task is easier than searching nonlinear counterexamples directly since the NN's behavior is summarized by the affine mapping ω . Using the definitions from the following subsections, this procedure is sound and complete (see proof on page 27):

B.1 Linearization

The procedure LINEARIZE enriches each nonlinear atom a_i of an open-loop NNV query with linear approximations. The approximations are always with respect to a value range R and we use overapproximations \overline{a}_i (for any state ν with $\nu \models a_i \wedge R$ it holds that $\nu \models \overline{a}_i$) as well as underapproximations \underline{a}_i (for any state ν with $\nu \models \underline{a}_i \wedge R$ it holds that $\nu \models a_i$). Essential to this component is the idea that LINEARIZE produces an equivalent formula: Approximate atoms do not replace, but complement the nonlinear atoms and the generation of concrete linear regions is left to the mosaic step (see Appendix B.2). LINEARIZE is defined as follows:

Definition 5 (Linearization). LINEARIZE receives an open-loop NNV query p with nonlinear atoms a_1, \dots, a_k and value range R s.t. $p \rightarrow R$ is valid. It returns a query $p \wedge \bigwedge_{i=1}^k ((a_i \rightarrow \overline{a}_i) \wedge (\underline{a}_i \rightarrow a_i))$

where $\overline{a_i} \in \text{FOL}_{\mathbb{L}\mathbb{R}}$ (resp. $\underline{a_i} \in \text{FOL}_{\mathbb{L}\mathbb{R}}$) are overapproximations (resp. underapproximations) of a_i w.r.t. R .

We use an approximation procedure based on OVERT [85] while further approximating max / min terms within OVERT. This results in a disjunction of linear constraints (see below for details). As highlighted above, LINEARIZE produces equivalent formulas and therefore retains the relations between linear and nonlinear atoms (see proof on page 27):

Lemma 6 (Equivalence of Linearization). *Let $p \in \text{FOL}_{\mathbb{R}}$ be some open-loop NNV query and p_o be the result of LINEARIZE(p). Then p is equivalent to p_o .*

Approximation. For conciseness we present our approximation approach for over-approximations. Our under-approximations are computed in the same manner, however lower and upper bound computation of terms is flipped in this case. We can approach the question of overapproximation construction from a perspective of models: For a given formula ζ , let $\llbracket \zeta \rrbracket = \{\nu \in \mathcal{S} \mid \nu \models \zeta\}$ be the set of models (i.e. states satisfying ζ). We then obtain the following Lemma for the relation between overapproximations and model sets:

Lemma 7 (Supersets are Overapproximations). *Assume bounds B on all variables and a formula ζ . Another formula $\zeta_o \in \text{FOL}_{\mathbb{L}\mathbb{R}}$ is a linear overapproximation of ζ iff $\llbracket B \wedge \zeta \rrbracket \subseteq \llbracket B \wedge \zeta_o \rrbracket$.*

This presentation only considers the case of a polynomial constraint $\theta > 0$. Our approximation procedure begins by computing the relational approximation of θ using the OVERT algorithm [85]. By resolving intermediate variables introduced through OVERT, we obtain an approximation of the form $\underline{\theta}_{pwl} \leq \theta \leq \overline{\theta}_{pwl}$ where both bounds are piece-wise linear functions (i.e. linear real arithmetic with the addition of max and min operators). It then holds that $\llbracket B \wedge \theta > 0 \rrbracket \subseteq \llbracket B \wedge \overline{\theta}_{pwl} > 0 \rrbracket$. We now distinguish between univariate and multivariate piece-wise linear behavior: For univariate piece-wise linear behavior there is some variable $v \in \mathcal{V}(\overline{\theta}_{pwl})$ and some coefficient $c \in \mathbb{R}$ with terms θ_1, θ_2 such that $\llbracket B \wedge \overline{\theta}_{pwl} > 0 \rrbracket = \llbracket B \wedge \overline{\theta}_1 > 0 \wedge v > c \rrbracket \cup \llbracket B \wedge \overline{\theta}_2 > 0 \wedge v \leq c \rrbracket$. In order to subsume piece-wise linear splits along variable v which are close to c , we construct the following overapproximation for a small $\varepsilon > 0$ resulting in two normalized queries:

$$\llbracket B \wedge \overline{\theta}_{pwl} > 0 \rrbracket \subseteq \llbracket B \wedge \overline{\theta}_1 > 0 \wedge v > (c - \varepsilon) \rrbracket \cup \llbracket B \wedge \overline{\theta}_2 > 0 \wedge v \leq (c + \varepsilon) \rrbracket.$$

For the multivariate cases we approximate the piece-wise linear behavior. In particular, we introduce a (to the best of our knowledge) novel, closed-form upper bound for the linear approximation of max terms:

Lemma 8 (Upper Bound for multivariate max). *Let $f, g : \mathbb{R}^{I+O} \rightarrow \mathbb{R}$ be two linear functions, and let $B \subset \mathbb{R}^{I+O}$ be a closed interval box, then: Assume $x_g := \arg \max_{x \in B} g(x) - f(x)$ and $x_f := \arg \max_{x \in B} f(x) - g(x)$ where $f(x_f) - g(x_f)$ and $g(x_g) - f(x_g)$ are both positive. Further, assume the following assignments with $\gamma := f(x_f) - f(x_g) - g(x_f) + g(x_g)$:*

$$\mu := -\frac{g(x_f) - f(x_f)}{\gamma} \quad c := -\frac{(f(x_f) - g(x_g))(f(x_g) - g(x_g))}{\gamma}.$$

In this case, it holds for all $x \in B$ that: $\mu f(x) + (1 - \mu)g(x) + c \geq \max(f(x), g(x))$. In particular, it holds that

$$\llbracket B \wedge (\max(f(x), g(x)) > 0) \rrbracket \subseteq \llbracket B \wedge ((\mu f(x) + (1 - \mu)g(x) + c) > 0) \rrbracket$$

Proof. At first, the choices for μ and c may seem arbitrary, however they are actually the solution of the following set of equations:

$$\begin{aligned} \mu f(x_f) + (1 - \mu)g(x_f) + c &= f(x_f) \\ \mu f(x_g) + (1 - \mu)g(x_g) + c &= g(x_g) \end{aligned}$$

The choice of μ and c ensures that we obtain a shifted convex mixture of the two linear functions that matches f and g at their points of maximal deviation. We can now prove that this shifted mixture is indeed larger than f or g at any point within B . Let us begin by proving that our bound is larger than

g for $x \in B$. In the following each formula implies the validity of the formula above:

$$\begin{aligned}
g(x) &\leq \mu f(x) + (1 - \mu)g(x) + c \\
0 &\leq \mu(f(x) - g(x)) + c \\
0 &\leq -\frac{1}{\gamma}((g(x_f) - f(x_f)) \underbrace{(f(x) - g(x))}_{\leq f(x_f) - g(x_f) \text{ for } x \in B}) + (f(x_f) - g(x_g))(f(x_g) - g(x_g))) \\
0 &\leq -\frac{1}{\gamma}((g(x_f) - f(x_f))(f(x_f) - g(x_f)) + (f(x_f) - g(x_g))(f(x_g) - g(x_g))) \\
0 &\leq \frac{1}{\gamma}(f(x_f) - g(x_f))\gamma \Leftrightarrow g(x_f) \leq f(x_f)
\end{aligned}$$

$g(x_f) \leq f(x_f)$ is trivially true since x_f was specifically chosen this way. We also have to prove that our bound is bigger than f for $x \in B$:

$$\begin{aligned}
f(x) &\leq \mu f(x) + (1 - \mu)g(x) + c \\
0 &\leq \underbrace{(g(x) - f(x))}_{\geq g(x_f) - f(x_f) \text{ for } x \in B} + \underbrace{\mu(f(x) - g(x)) + c}_{\geq f(x_f) - g(x_f) \text{ (see previous proof)}} \\
0 &\leq g(x_f) - f(x_f) + f(x_f) - g(x_f) = 0
\end{aligned}$$

Thus we obtain an upper bound for the function. \square

By applying OVERT followed by the univariate resolution and multivariate overapproximation up to saturation, we compute an overapproximation and underapproximation for each nonlinear atom. Subsequently, we append these new formulas to the original formula as defined in Definition 5.

Running Example. The turquoise constraints in Figure 3 visualize exemplary linearized constraints. For ACC one nonlinear atom is $p_{rel} - \frac{v_{rel}^2}{2B} \geq 0$. The formula $\text{accApprox} \equiv p_{rel} - \frac{100^2}{2B} \geq 0 \wedge v_{rel} > 50 \vee v_{rel} \leq 50 \wedge p_{rel} - \frac{50^2}{2B} \geq 0$ underapproximates the atom for $v_{rel} \in [0, 100]$. We can thus append the following formula to our query: $(\text{accApprox} \rightarrow p_{rel} - \frac{v_{rel}^2}{2B} \geq 0)$. For $v_{rel} \in [0, 100]$ this formula is always satisfied⁴.

B.2 Input Space Mosaics

The MOSAIC procedure takes a central role in the verification of nonlinear, non-normalized open-loop NNV queries. Classically, one uses DPLL(T) to decompose an arbitrary formula into conjunctions then handled by a theory solver. Open-loop NNV's crux is its use of reachability methods which do not lend themselves well to *classic* DPLL(T): Its usage would result in duplicate explorations of the same input space w.r.t. different output constraints which is inefficient. Therefore, we generalize DPLL(T) [38] through the MOSAIC procedure. The procedure receives a quantifier-free⁵, non-normalized open-loop NNV query and enumerates *azulejos* of the input space each with an associated normalized linear open-loop NNV query q_l (conjunction over input atoms, disjunctive normal form over output atoms) and nonlinear atoms in disjunctive normal form q_n . The input space is thus turned into a mosaic and the disjunction over all queries is *equivalent* to the input query. We can then obtain classical DPLL(T) by marking all atoms as linear input constraints. Our implementation of MOSAIC instruments a SAT solver on the Boolean skeleton of p as well as a real arithmetic SMT solver to restructure a formula in this way.

For a formula $\zeta \in \text{FOL}_{\mathbb{R}}$, let $\text{sat-atoms}(\zeta)$ be the set of set of signed atoms such that for all $A \in \text{sat-atoms}(\zeta)$ it holds that A only contains atoms of ζ or its negations ($A \subseteq \text{Atom}(\zeta) \cup \{-b \mid b \in \text{Atom}(\zeta)\}$). Further, we require for $\text{sat-atoms}(\zeta)$ that for any state ν it holds that $\nu \models \zeta$ iff there exists an $A \in \text{sat-atoms}(\zeta)$ such that $\nu \models \bigwedge_{a \in A} a$. Note that there may exist multiple such sets in which case we can choose an arbitrary one. For example, for $\zeta \equiv x > 0 \vee \neg(y > 0)$ we could get

⁴In practice, v_{rel} may also be negative requiring a more complex approximation.

⁵A quantifier-free p can be assumed as real arithmetic admits quantifier elimination [87]. In practice, all queries of interest were already quantifier-free.

$\text{sat-atoms}(\zeta) = \{\{x > 0\}, \{\neg(x > 0)\}, \neg(y > 0)\}$. For a given formula ζ , we will call J_ζ the set of input variables. We introduce the following notation for projection of sat-atoms on the set J_ζ :

$$\text{sat-atoms}(\zeta) \downarrow_{J_\zeta} = \{\{a \mid a \in A \wedge \forall(a) \subseteq J_\zeta\} \mid A \in \text{sat-atoms}(\zeta)\}.$$

For example, reconsidering the previous example with $J_\zeta = \{x\}$ we would get $\text{sat-atoms}(\zeta) \downarrow_{J_\zeta} = \{\{x > 0\}, \{\neg(x > 0)\}\}$. For a given open-loop NNV query p_o and a given set of input variables J_{p_o} , MOSAIC then initially enumerates feasible combinations of linear input atoms (the azulejos) and for each such combination feasible combinations of mixed/output atoms are enumerated. This results in the following set:

$$S_1 = \left\{ \left(\bigwedge_{\substack{a \in i \\ a \in \text{FOL}_{\text{LR}}}} a \right) \wedge \left(\bigvee_{o \in \text{sat-atoms}(p_o \wedge i)} \left(\bigwedge_{\substack{b \in o \\ b \in \text{FOL}_{\text{LR}}}} b \right) \right) \mid i \in \text{sat-atoms}(p_o) \downarrow_{J_{p_o}} \right\}$$

Finally, for each $q_l \in S_1$, we can generate all possible combinations of nonlinear atoms $S_2 = \text{sat-atoms}(p_o \wedge q_l)$ and generate their disjunction:

$$q_n \equiv \bigvee_{A \in S_2} \bigwedge_{a \in A} a \quad (7)$$

We achieve this by enumerating all satisfying assignments for the boolean skeleton of p_o (i.e. the formula where all atoms are substituted by boolean variables) using an incremental SAT solver. This initially happens in the same manner as it is done for the classical version of DPLL(T). However, once a model is found, we fix the assignment of linear input-only atoms and enumerate all other satisfying assignments of linear atoms, generating the disjunctions within S_1 . For each conjunction we additionally enumerate possible assignments for the nonlinear atoms. Notably, through the encoding of LINEARIZE the procedure automatically knows which truth-combinations of a nonlinear constraint and its approximations may appear. We additionally provide information on linear dependencies between linear atoms to the SAT solver. All enumeration procedures are interleaved with calls to SMT solvers for linear and polynomial real arithmetic constraints, which check whether a given combination of constraints is indeed also satisfiable in the theory of real arithmetic (i.e. when interpreting the atoms as real arithmetic constraints instead of as boolean variables). In order to discard unsatisfiable solutions more quickly, we make use of unsatisfiability cores and conversely use a cache for satisfiable assignment combinations. We exploit partial models returned by the SAT solver to omit atoms which can (potentially) appear in both polarities for a given combination of constraints.

We show that the decomposition is correct (i.e. the disjunction over all queries is equivalent to the original query, see Proposition 9) and that it is minimal in the sense that the resulting azulejos do not overlap (see Proposition 10) with proofs on page 27:

Proposition 9 (Correctness of Mosaic). *Let p be any open-loop NNV query. Let $Q \subset \text{FOL}_{\text{LR}} \times \text{FOL}_{\text{R}}$ be the set returned by MOSAIC(p), then the following formula is valid: $p \leftrightarrow (\bigvee_{(q_l, q_n) \in Q} (q_l \wedge q_n))$*

Proposition 10 (Flatness of Mosaic). *Let $(i_1 \wedge \bigvee_j o_{1,j}), (i_2 \wedge \bigvee_j o_{2,j})$ be two linear queries enumerated by MOSAIC then $i_1 \wedge i_2$ is unsatisfiable.*

We could use this approach to decompose a nonlinear formula into a set of normalized linear open-loop NNV queries without approximation. MOSAIC then soundly omits all nonlinear constraints. However, this leads to many spurious counterexamples. Therefore, we add linear approximations (Appendix B.1) of atoms which are then automatically part of the conjunctions returned by MOSAIC.

Running Example. In the previous section we extended our query by a linear underapproximation. Our procedure generates an azulejo for the case where $p_{rel} - \frac{100^2}{2B} \geq 0 \wedge v_{rel} > 50$ is satisfied (implying $p_{rel} - \frac{v_{rel}^2}{2B} \geq 0$) and the case where it is not. While the linear approximation is an edge of the mosaic tile, the original atom (the tile’s “painting” describing the precise constraint) would be part of the *nonlinear* disjunctive normal form. For each azulejo, the output conjunctions of accCtrlFml are enumerated. For OVERT’s approximation with $N = 1$, our implementation decomposes the ACC query into 20 normalized queries with up to 10 cases in the output constraint disjunction. Without MOSAIC each case would be treated as a separate reachability query leading to significant duplicate work.

Relation to DPLL(T) Abstracting away the real-arithmetic, the MOSAIC algorithm generates tuples of normalized open-loop NNV queries and disjunctive normal forms that are satisfiable w.r.t. a theory solver T . The algorithm itself interleaves SAT-based reasoning about a boolean abstraction (annotated with information on whether an atom is linear and/or an input constraint) and theory solver invocations. We can now consider the case where all atoms (independent of their concrete contents and the theory T) are annotated as linear input constraints: In this case MOSAIC merely returns a mosaic of this “input” space where each azulejo corresponds to a conjunction of atoms that is satisfiable w.r.t. to the theory solver T and the disjunction over all those conjunctions is then once again equivalent to the original formula – corresponding to DPLL(T)’s behavior.

B.3 Counterexample Generalization and Enumeration

The innermost component of our algorithm enumerates all counterexample regions (ENUM). To this end, ENUM requires an algorithm which generalizes counterexample *points* returned by open-loop NNV to *regions* (GENERALIZE). For each such counterexample region we can then check if there exist concrete violations of the nonlinear constraints (FILTER). We begin by explaining GENERALIZE which converts a counterexample point returned by open-loop NNV into a counterexample region. The key insight for this approach is that a concrete counterexample (z_0, x_0) returned by an open-loop NNV tool induces a region of points with *similar behavior* in the NN. A concrete input z_0 induces a fixed activation pattern for all piece-wise linear activations within the NN in a region ι around z_0 . Consider the first layer’s activation function $f^{(1)}$: $f^{(1)}$ can be decomposed into linear functions f_i and so is a sum of affine transformations $A_i z_0 + b_i$ which are active iff $q_i(z_0)$ is true. We can then describe $f^{(1)}$ ’s local behavior around z_0 as the linear combination of all affine transformations active for z_0 . This sum is itself an affine transformation. By iterating this approach across layers, we obtain a single affine transformation ω describing the NN’s behavior in ι . The regions returned by GENERALIZE are then defined as follows:

Definition 11 (Counterexample Region). *For a given open-loop NNV query q and piece-wise linear NN g , let $(z_0, x_0) \in \mathbb{R}^I \times \mathbb{R}^O$ be a counterexample, i.e. $x_0 = g(z_0)$ and $q(z_0, x_0)$ holds. The counterexample region for z_0 is the maximal polytope $\iota \subset \mathbb{R}^I$ with a linear function ω s.t. $z_0 \in \iota$ and $\omega(z) = g(z)$ for all $z \in \iota$.*

Star Sets [11, 88] can compute (ι, ω) by steering the Star Set according to the activations of z_0 . As the number of counterexample regions is exponentially bounded by the number of piece-wise linear nodes, we can use GENERALIZE for exhaustive enumeration. This is only a worst-case bound due to the NP-completeness of NN verification [56, 81]. In practice, the number of regions is much lower since many activation functions are linear in all considered states. While a given counterexample region certainly has a point violating the *linear* query that was given to the open-loop NNV tool, it may be the case that the counterexample is *spurious*, i.e. it does not violate the nonlinear constraints. However, we can use the concise description of counterexample regions to check whether this is the case: The function ω describes the NN’s *entire* behavior within ι as a single affine transformation and is thus much better suited for SMT-based reasoning. This SMT-based check is performed by FILTER based on the following insight:

Lemma 12 (Counterexample Filter). *Let (q_l, q_n) be a tuple returned by MOSAIC. A counterexample region (ι, ω) for q_l is a counterexample region for $q_l \wedge q_n$ iff the formula $\eta \equiv (q_l(z, x^+) \wedge q_n(z, x^+) \wedge z \in \iota \wedge x^+ = \omega(z))$ is satisfiable.*

See proof on page 27. The size of the formula η only depends on q_l, q_n, I , and O and, crucially, is *independent* of the size and architecture of the NN. In practice, even x^+ can be eliminated (substitute linear terms of $\omega(x^+)$).

Based on these insights, the last required component is a mechanism for the exhaustive enumeration of all counterexample regions (denoted as ENUM). There are two options for ENUM: Either we use geometric path enumeration [11, 88] to enumerate all counterexample regions (used for the evaluation) or we instrument arbitrary complete off-the-shelf open-loop NNV tools for linear queries through Algorithm 2. We define ENUM as follows:

Definition 13 (Exhaustive Counterexample Generation). *An exhaustive enumeration procedure ENUM receives a linear, normalized open-loop NNV query q and a piece-wise linear NN g and returns a covering E of counterexample regions, i.e. E satisfies $\{z \in \mathbb{R}^I \mid q(z, g(z))\} \subseteq \bigcup_{(\iota, \omega) \in E} \iota$.*

Algorithm 2: Enumeration of counterexample regions using off-the-shelf open-loop NNV tools.

Input: Query \bar{p} , feed forward neural network (FNN) g

```

procedure ENUMERATE( $\bar{p}, g$ )
   $s, E \leftarrow \text{sat}, \emptyset$ 
  while  $s = \text{sat}$  do
     $s, e \leftarrow \text{NNV}(\bar{p}, g)$  ▷ Call open-loop NNV tool
    if  $s = \text{sat}$  then
       $\iota, \omega \leftarrow \text{GENERALIZE}(e, g)$  ▷ Generalize counterexample
       $E \leftarrow E \cup \{(\iota, \omega)\}$  ▷ Store counterexample
       $\bar{p} \leftarrow \bar{p} \wedge \neg \iota$  ▷ Exclude counterexample region from remaining search space
  return  $E$ 

```

C Proofs

C.1 Proofs for Section 3

This subsection proves the soundness of the approach outlined in Section 3. This result is achieved by proving that a concrete NNCS refines [63, 76] an abstract hybrid program. The approach can either be applied by first proving safety for a suitable $d\mathcal{L}$ model or by reusing results from the $d\mathcal{L}$ literature (both demonstrated Section 5 and appendix E). In our proofs for Section 3 we show a slightly more general version of the result from Theorem 2 (see Theorem 21). To this end, we formally define a controller description as follows:

Definition 14 (Controller Description). *Let α_{ctrl} be some hybrid program with free variables $FV(\alpha_{ctrl}) = \{z_1, \dots, z_m\}$ and bound variables $BV(\alpha_{ctrl}) = \{x_1, \dots, x_n\}$, which overlap if a variable is both read and written to. A controller description $\kappa \in \text{FOL}_{\mathbb{N}\mathbb{R}}$ for α_{ctrl} is a formula with free variables $FV(\alpha_{ctrl}) \cup \{x^+ \mid x \in BV(\alpha_{ctrl})\}$ such that the following formula is valid: $\forall z_1 \dots z_m \exists x_1^+ \dots x_n^+ \kappa$.*

Based on Controller Descriptions we can then show that such controller descriptions exist for all piece-wise Noetherian NNs:

Lemma 15 (Existence of κ_g). *Let $g : \mathbb{R}^I \rightarrow \mathbb{R}^O$ be a piece-wise Noetherian NN. There exists a controller description $\kappa_g \in \text{FOL}_{\mathbb{N}\mathbb{R}}$ with input variables z_1, \dots, z_I and output variables x_1^+, \dots, x_O^+ s.t. $(\nu(x_1^+), \dots, \nu(x_O^+)) = g(\nu(z_1), \dots, \nu(z_I))$ iff $\nu \models \kappa_g$, i.e. κ_g 's satisfying assignments correspond exactly to g 's in-out relation.*

Proof. Previous work showed how to encode piece-wise linear NNs through real arithmetic SMT formulas (see e.g. [34, 69]). Each output dimension of an affine transformation can be directly encoded as a real arithmetic term. For a given output-dimension of a piece-wise Noetherian activation function we have to encode a term $\sum_{i=1}^s \mathbb{1}_{q_i}(x) f_i(x)$ with Noetherian functions f_i and predicates q_i over real arithmetic with Noetherian functions. To this end, we can introduce fresh variables v_1, \dots, v_s where we assert the following formula for each v_i :

$$(q_i \wedge v_i = f_i(x)) \vee (\neg q_i \wedge v_i = 0).$$

The activation function's result then is the sum $\sum_{i=1}^s v_i$. By existentially quantifying all intermediate variables of such encodings, we obtain a real arithmetic formula that only contains input and output variables and satisfies the requirements of the Lemma.

If we assign $x_1^+ \dots x_O^+$ to the values provided by $g(z_1, \dots, z_I)$ for a given $z_1 \dots z_I$, the formula κ_g is satisfied. Therefore, $\forall z_1 \dots z_I \exists x_1^+ \dots x_O^+ \kappa_g$ is valid. \square

When replacing α_{ctrl} by an NN g , free and bound variables of α_{ctrl} must resp. match to input and output variables of g . Based of a description κ_g , we then construct a hybrid program that behaves as described by κ_g : We now formalize the idea of modeling a given NN g through a hybrid program which behaves identically to g . We show that such *nondeterministic mirrors exist* for all piece-wise Noetherian NN g :

Definition 16 (Nondeterministic Mirror for κ_g). *Let α_{ctrl} be some hybrid program with bound variables $BV(\alpha_{ctrl}) = \{x_1, \dots, x_n\}$. For a controller description κ_g with variables matching to α_{ctrl} ,*

κ_g 's nondeterministic mirror α_{refl} is defined as:

$$\alpha_{\text{refl}}(\kappa_g) \equiv (x_1^+ := *; \dots; x_n^+ := *; ?(\kappa_g); x_1 := x_1^+; \dots; x_n := x_n^+)$$

Lemma 17 (Existence of α_g). *For any piece-wise Noetherian NN $g : \mathbb{R}^I \rightarrow \mathbb{R}^O$ there exists a nondeterministic mirror α_g that behaves identically to g .*

Formally, α_g only has free variables \bar{z} and bound variables \bar{x} and for any state transition $(\nu, \mu) \in \llbracket \alpha_g \rrbracket$: $\mu(\bar{x}) = g(\nu(\bar{z}))$ (\bar{x} and \bar{z} vectors of dimension I and O)

Proof. Based on Lemma 15 we can construct a controller description $\kappa_g \in \text{FOL}_{\text{N}\mathbb{R}}$ for g which we can turn into a hybrid program through the nondeterministic mirror $\alpha_{\text{refl}}(\kappa_g)$. \square

Similarly to the more general notion of a controller description, Theorem 21 also permits a slightly more general version of a state space restriction instead of an inductive invariant. Formally, this notion is described as a state reachability formula:

Definition 18 (State Reachability Formula). *A state reachability formula ζ_s with free variables z_1, \dots, z_m is complete for the hybrid program $(\alpha_{\text{ctrl}}; \alpha_{\text{plant}})^*$ with free variables z_1, \dots, z_m and initial state ϕ iff the following $d\mathcal{L}$ formula is valid where $(\zeta_s)_{z_1 \dots z_m}^{z_1^+ \dots z_m^+}$ represents ζ_s with z_i^+ substituted for z_i for all $1 \leq i \leq m$:*

$$\left(\phi \wedge \langle (\alpha_{\text{ctrl}}; \alpha_{\text{plant}})^* \rangle \bigwedge_{i=1}^m z_i = z_i^+ \right) \rightarrow (\zeta_s)_{z_1 \dots z_m}^{z_1^+ \dots z_m^+}. \quad (8)$$

There is usually an overlap between free and bound variables, i.e. z_1, \dots, z_m may contain variables later modified by the hybrid program. Our definition requires that for any program starting in a state satisfying ϕ , formula ζ_s is satisfied in all terminating states. ζ_s thus overapproximates the program's reachable states. In particular, inductive invariants (i.e. for $\phi \rightarrow [\alpha^*] \psi$ a formula ζ s.t. $\phi \rightarrow \zeta$ and $\zeta \rightarrow [\alpha] \zeta$) are state reachability formulas:

Lemma 19 (Inductive Invariants are State Reachability Formulas). *If ζ is an inductive invariant of $\phi \rightarrow [(\alpha_{\text{ctrl}}; \alpha_{\text{plant}})^*] \psi$, ζ is a state reachability formula.*

Proof. We begin by recalling the requirement for ζ to be a state reachability formula:

$$\left(\phi \wedge \langle (\alpha_{\text{ctrl}}; \alpha_{\text{plant}})^* \rangle \bigwedge_{i=1}^m z_i = z_i^+ \right) \rightarrow (\zeta_s)_{z_1 \dots z_m}^{z_1^+ \dots z_m^+}.$$

Let ζ be an inductive invariant for some contract of the form given above. First, consider that for any state satisfying the left side of the formula above it holds that there exists some k such that $\phi \wedge \langle (\alpha_{\text{ctrl}}; \alpha_{\text{plant}})^k \rangle \bigwedge_{i=1}^m z_i = z_i^+$ is satisfied by the same state (this follows from the semantics of loops in $d\mathcal{L}$). If we can prove that any such state also satisfies $(\zeta_s)_{z_1, \dots, z_m}^{z_1^+, \dots, z_m^+}$ we obtain that ζ is a state reachability formula. We proceed by induction: First, consider $k = 0$ in this case z_i has the same value as z_i^+ for all i . The formula then boils down to $\phi \rightarrow \zeta$. This formula is guaranteed to be valid by the first requirement of inductive invariants. Next, we now assume that we already proved that ζ holds for k loop iterations and show it for $k + 1$. Since we assume some state u_{k+1} that satisfies $\phi \wedge \langle (\alpha_{\text{ctrl}}; \alpha_{\text{plant}})^{k+1} \rangle \bigwedge_{i=1}^m z_i = z_i^+$, there also has to be some state u_k satisfying $\phi \wedge \langle (\alpha_{\text{ctrl}}; \alpha_{\text{plant}})^k \rangle \bigwedge_{i=1}^m z_i = z_i^+$. However, we already know for u_k that it satisfies $(\zeta_s)_{z_1, \dots, z_m}^{z_1^+, \dots, z_m^+}$. Since u_{k+1} is reachable from u_k through the execution of $\alpha_{\text{ctrl}}; \alpha_{\text{plant}}$ we know that u_{k+1} satisfies $(\zeta_s)_{z_1, \dots, z_m}^{z_1^+, \dots, z_m^+}$ (this corresponds to the property $\zeta \rightarrow [\alpha] \zeta$ of inductive invariants). \square

As α_g and g mirror each other, we can reason about them interchangeably. Our objective is now to prove that α_g is a refinement of α_{ctrl} . To this end, we use the shielding technique ModelPlex [66] to automatically generate a correct-by-construction controller monitor ζ_c for α_{ctrl} . The formula ζ_c then describes what behavior for α_g is acceptable so that α_g still represents a refinement of α_{ctrl} . As seen in Section 3, we do *not* require that α_g adheres to ζ_c on all states, but only on reachable states. For efficiency we therefore allow limiting the analyzed state space to an inductive invariant ζ_s (i.e. for $\phi \rightarrow [\alpha^*] \psi$ a formula ζ_s s.t. $\phi \rightarrow \zeta_s$ and $\zeta_s \rightarrow [\alpha] \zeta_s$). Despite the infinite-time horizon, the practical use of our approach often faces implementations with a limited value range for inputs and outputs (e.g.,

v_{rel} within the ego-car's physical capabilities). Only by exploiting these ranges, is it possible to prove safety for NNs that were only trained on a particular value range. To this end, we allow specifying value *ranges* (i.e. intervals) for variables. We define the range formula $R \equiv \bigwedge_{v \in V(P)} \underline{R}(v) \leq v \leq \overline{R}(v)$ for lower and upper bounds \underline{R} and \overline{R} . Using R , we specialize a contract to the implementation specifics by adding a range check to α_{plant} . The safety results for the original contract can be reused:

Lemma 20 (Range Restriction). *Let $\phi \rightarrow [(\alpha_{ctrl}; \alpha_{plant})^*] \psi$ be a valid $d\mathcal{L}$ formula. Then the formula $C_2 \equiv (\phi \wedge R \rightarrow [(\alpha_{ctrl}; (\alpha_{plant}; ?(R)))^*] \psi)$ with ranges R is valid and R is an invariant for C_2 .*

Proof. We use the notation $C_1 \equiv (\phi \rightarrow [(\alpha_{ctrl}; \alpha_{plant})^*] \psi)$. We begin by showing that the validity of C_1 implies the validity of C_2 . Intuitively, this follows from the fact that the introduced check $?(R)$ only takes away states. Let I be a loop invariant such that $\phi \rightarrow I$, $I \rightarrow \psi$ and $I \rightarrow [(\alpha_{ctrl}; \alpha_{plant})] I$ (assumed due to the validity of C_1). Then clearly, it also holds that $\phi \wedge R \rightarrow I$. Furthermore, $I \rightarrow [(\alpha_{ctrl}; \alpha_{plant}; ?(R))] I$ can be reduced to $I \rightarrow [(\alpha_{ctrl}; \alpha_{plant})] (R \rightarrow I)$ which we can show through the monotonicity rule of $d\mathcal{L}$. Since we already know that $I \rightarrow \psi$, it follows that C_2 is valid, because I is a loop invariant. \square

Including R into ζ_s allows us to exploit the range limits for the analysis of α_g . Our objective is to use open-loop NNV techniques to check whether g (and therefore α_g) satisfies the specification synthesized by ModelPlex. To this end, we use a *nonlinear NN verifier* to prove safety of our NNCS:

Theorem 21 (Safety Criterion). *Let ζ_c and ζ_s be controller and state reachability formulas for a valid $d\mathcal{L}$ contract $C \equiv (\phi \rightarrow [(\alpha_{ctrl}; \alpha_{plant})^*] \psi)$. For any controller description κ , if*

$$\zeta_s \wedge \kappa \rightarrow \zeta_c \quad (9)$$

is valid, then the following $d\mathcal{L}$ formula is valid as well:

$$\phi \rightarrow [(\alpha_{refl}(\kappa); \alpha_{plant})^*] \psi \quad (10)$$

Proof. Assume the validity of

$$\zeta_s \wedge \kappa \rightarrow \zeta_c.$$

Let $v \in \mathcal{S}$ be some arbitrary state. We need to show that any such v satisfies Formula (10):

$$\phi \rightarrow [(\alpha_{refl}(\kappa); \alpha_{plant})^*] \psi.$$

To this end, assume $v \models \phi$, we prove that ψ as well as ζ_s is upheld after any number of loop iterations by induction on the number n of loop iterations.

Base Case: $n = 0$

In this case, the only state we need to consider is v since there were no loop iterations. We know through the validity of C that $\phi \rightarrow \psi$. Thus, $v \models \psi$. Furthermore, we recall the requirement of a state reachability formula:

$$\left(\phi \wedge \left((\alpha_{ctrl}; \alpha_{plant})^* \right) \bigwedge_{i=1}^m z_i = z_i^+ \right) \rightarrow (\zeta_s)_{z_1^+ \dots z_m^+}.$$

By extending v such that all z_i^+ have the same values as the corresponding z_i , we get a state that satisfies this formula. Consequently, $v \models \zeta_s$.

Inductive Case: $n \rightarrow (n + 1)$

In the induction case, we know that for all

$$(v, \tilde{v}_0) \in \left[\left[(\alpha_{refl}(\kappa); \alpha_{plant})^n \right] \right]$$

it holds that $\tilde{v}_0 \models \psi$ and $\tilde{v}_0 \models \zeta_s$.

We must now prove the induction property for any state reachable from \tilde{v}_0 through execution of the program $(\alpha_{refl}(\kappa); \alpha_{plant})$. For any $\tilde{v}_1 \in \mathcal{S}$ such that $(\tilde{v}_0, \tilde{v}_1) \in \left[\left[x_1^+ := *; \dots; x_n^+ := *; ?(\kappa); \right] \right]$ (by the

definition of κ we know that such a state exists) we know that $\tilde{v}_1 \models \kappa$. According to the coincidence lemma [66, Lemma 3], since ζ_s does not concern the x^+ variables, it is then true that

$$\tilde{v}_1 \models \zeta_s \wedge R \wedge \kappa.$$

Through the validity of Formula (9) assumed at the beginning, we then know that it must be the case that $\tilde{v}_1 \models \zeta_c$. More specifically, this means that for any $\tilde{v}_2 \in \mathcal{S}$ with

$$(\tilde{v}_1, \tilde{v}_2) \in \llbracket x_1 := x_1^+; \dots; x_n := x_n^+ \rrbracket;$$

it holds that $(\tilde{v}_0, \tilde{v}_2) \models \zeta_c$. By definition this implies that $(\tilde{v}_0, \tilde{v}_2) \in \llbracket \alpha_{\text{ctrl}} \rrbracket$.

In summary, this means that for any $(\tilde{v}_0, \tilde{v}_2) \in \llbracket \alpha_{\text{refl}}(\kappa) \rrbracket$ it holds that $(\tilde{v}_0, \tilde{v}_2) \in \llbracket \alpha_{\text{ctrl}} \rrbracket$.

Through the semantics of program composition in hybrid programs it follows that subsequently for any $\tilde{v}_3 \in \mathcal{S}$ with $(\tilde{v}_0, \tilde{v}_3) \in \llbracket \alpha_{\text{refl}}(\kappa); \alpha_{\text{plant}} \rrbracket$ it holds that $(\tilde{v}_0, \tilde{v}_3) \in \llbracket \alpha_{\text{ctrl}}; \alpha_{\text{plant}} \rrbracket$.

We also know that $(v, \tilde{v}_0) \in \llbracket (\alpha_{\text{ctrl}}; \alpha_{\text{plant}})^* \rrbracket$ and that $(\tilde{v}_0, \tilde{v}_3) \in \llbracket \alpha_{\text{ctrl}}; \alpha_{\text{plant}} \rrbracket$. Since this implies $(v, \tilde{v}_3) \in \llbracket (\alpha_{\text{ctrl}}; \alpha_{\text{plant}})^* \rrbracket$, i.e. there is a trace of states from v to \tilde{v}_3 , and since we already know that $v \models \phi$, (v, \tilde{v}_3) satisfy the right side of Formula (8). Since Formula (8) must be valid we get that $\tilde{v}_3 \models \zeta_s$. Consequently, we know through the validity of C that:

$$\tilde{v}_3 \models \psi \wedge \zeta_s.$$

This concludes the induction proof and thereby also the proof of Theorem 21 □

Lemma 22 (Soundness w.r.t Controller Descriptions). *Let κ_g be a controller description for a piece-wise Noetherian NN g .*

Further, let $C \equiv (\phi \rightarrow [(\alpha_{\text{ctrl}}; \alpha_{\text{plant}})^] \psi)$ be a contract with controller monitor $\zeta_c \in \text{FOL}_{\mathbb{R}}$ and inductive invariant $\zeta_s \in \text{FOL}_{\mathbb{R}}$ where the free and bound variables respectively match g 's inputs and outputs. If a sound Nonlinear Neural Network Verifier returns *unsat* for the query $p \equiv (\zeta_s \wedge \neg \zeta_c)$ on g then: 1. $\kappa_g \wedge \zeta_s \rightarrow \zeta_c$ is valid; 2. $\phi \rightarrow [(\alpha_{\text{refl}}(\kappa_g); \alpha_{\text{plant}})^*] \psi$ is valid.*

Proof. Let all variables be defined as above. We assume that the nonlinear NN verifier did indeed return *unsat*. By definition this means that there exists no $z \in \mathbb{R}^I$ such that $p(z, g(z)) = \top$. Due to the formalization of κ_g (see Lemma 15), this means there exists no $z \in \mathbb{R}^I$ such that $\zeta_s \wedge R \wedge \kappa_g \wedge \neg \zeta_c$. Among all states consider now any state v such that $v \not\models \zeta_s \wedge R \wedge \kappa_g$. In this case $v \models \zeta_s \wedge R \wedge \kappa_g \rightarrow \zeta_c$ vacuously. Next, consider the other case, i.e. a state v such that $v \models \zeta_s \wedge R \wedge \kappa_g$. In this case it must hold that $v \not\models \neg \zeta_c$. So $v \models \zeta_c$. Therefore, $v \models \zeta_s \wedge R \wedge \kappa_g \rightarrow \zeta_c$. This means that Formula (9) is satisfied by all states and, therefore, valid which proves the first claim. Theorem 21 then implies the safety guarantee stated in Formula (10) for κ_g which proves the second claim. □

Definition 23 (Nonlinear Neural Network Verifier). *A nonlinear neural network verifier accepts as input a piece-wise Noetherian NN g and nonlinear open-loop NNV query p with free variables $z_1, \dots, z_I, x_1^+, \dots, x_n^+$. The tool must be sound, i.e. if there is a $z \in \mathbb{R}^I$ satisfying $p(x, g(z))$ then the tool must return *sat*. A tool that always returns *unsat* if no such $z \in \mathbb{R}^I$ exists is called complete.*

This means, that after replacing α_{ctrl} by g (or more specifically by α_g) safety (i.e. ψ) is guaranteed for arbitrarily many loop iterations. While this section lays the foundation for analyses on the general range of piece-wise Noetherian NNs, some subclasses are decidable (see proof on page 26):

Lemma 24 (Decidability for Polynomial Constraints). *Given a piece-wise polynomial NN g , the problem of verifying $(\zeta_s \wedge \neg \zeta_c) \in \text{FOL}_{\mathbb{R}}$ for g is decidable.*

Proof. The problem of verifying $(\zeta_s \wedge \neg \zeta_c) \in \text{FOL}_{\mathbb{R}}$ for g is the same as proving the validity of the formula $\zeta_s \wedge \kappa_g \rightarrow \zeta_c$ (see Lemma 22). For piece-wise polynomial NN this formula is in $\text{FOL}_{\mathbb{R}}$ and the validity problem is thus decidable. □

Proof of 2. The formula $\phi \rightarrow [(\alpha_g; \alpha_{\text{plant}})^*] \psi$ is equivalent to $\phi \rightarrow [(\alpha_{\text{refl}}(\kappa_g); \alpha_{\text{plant}})^*] \psi$ as α_g behaves precisely like $\alpha_{\text{refl}}(\kappa_g)$. Based on this insight the present result immediately follows from Lemma 22 □

C.2 Proofs for Section 4

Proof of 3. This proof assumes the results from Appendices B.1 to B.3. We begin by proving soundness, i.e. if Algorithm 1 returns `safe`, then there exists no counterexample. Consider a counterexample region found by ENUM. Lemma 12 tells us that this counterexample can only be concrete if formula ν is satisfied. This is the check performed by FILTER. Thus, Algorithm 1 only skips a counterexample region if it is not concrete. Further, we know through Definition 13 that all counterexamples are returned by the procedure for a given query q_l . Further, we know that the disjunction over all $q_l \wedge q_n$ returned by MOSAIC is equivalent to its input p_o (Proposition 9) and thus the disjunction over all q_l is an over-approximation thereof. Finally, LINEARIZE returns a formula p_o which is equivalent to the input query p (Lemma 6). Therefore, any counterexample of p must also be a counterexample of some q_l returned by MOSAIC. Consequently, Algorithm 1 iterates over all possible counterexamples and only discards them if they are indeed spurious. Thus, our algorithm is sound.

We now turn to the question of completeness, i.e. we prove that any time Algorithm 1 returns `unsafe` then there is indeed a concrete counterexample of p . First, remember that Lemma 6 ensures that p and p_o are equivalent. Furthermore, Proposition 9 ensures that the disjunction over all $q_l \wedge q_n$ generated by MOSAIC is equivalent to p_o . Assume we found a counterexample. The algorithm will return `unsafe` iff FILTER returns that the counterexample is concrete. According to Lemma 12 we know that this is only the case if there is indeed a concrete counterexample for $q_l \wedge q_n$. Since this counterexample then also satisfies p_o (see above), we only return `unsafe` if FILTER found a concrete counterexample for p . As real arithmetic is decidable and all other procedures in the algorithm terminate as well, this yields a terminating, sound and complete algorithm. \square

Proof of 6. Let $p \in \text{FOL}_{\mathbb{R}}$ be some nonlinear open-loop NNV query and a_1, \dots, a_k be the nonlinear atoms in p . From the definition of LINEARIZE, we know that p_o has the form $p \wedge \bigwedge_{i=1}^k ((a_i \rightarrow \bar{a}_i) \wedge (\underline{a}_i \rightarrow a_i))$. By definition, it holds for approximations $\underline{a}_i, \bar{a}_i$ that for any state ν with $\nu \models a_i \wedge R$ it also holds that $\nu \models \bar{a}_i$ (resp. for any state ν with $\nu \models \underline{a}_i \wedge R$ it also holds that $\nu \models a_i$). Consequently, the formulas $R \rightarrow (a_i \rightarrow \bar{a}_i)$ and $R \rightarrow (\underline{a}_i \rightarrow a_i)$ are valid for all a_i . Let ν be a state such that $\nu \models p$. Then, by definition $\nu \models R$ and due to the above mentioned validity it therefore holds that $\nu \models a_i \rightarrow \bar{a}_i$ and $\nu \models \underline{a}_i \rightarrow a_i$. Therefore, $\nu \models p_o$. Conversely, for any state with $\nu \models p_o$ it also holds that $\nu \models p$. \square

Proof of 9. We begin by considering the case where some state ν satisfies $\bigvee_{(q_l, q_n) \in Q} q_l \wedge q_n$. By definition, this means that there exists some $(q_l^*, q_n^*) \in Q$ such that $\nu \models q_l^* \wedge q_n^*$. Through the definition of the set S_1 in Appendix B, we know that q_l^* contains a conjunction over linear input atoms i_l^* . Let $o_l^* \in \text{sat-atoms}(p \wedge i_l^*)$ be the set of mixed/output atoms such that $\nu \models \bigwedge_{b \in o_l^*} b$. Further, since $\nu \models q_n^*$, we know there also exists an $A^* \in \text{sat-atoms}(p \wedge q_l^*)$ such that $\nu \models \bigwedge_{a^* \in A^*} a^*$. Through the definition of sat-atoms and its projection we then know that $A^* \cup i_l^* \cup o_l^* \in \text{sat-atoms}(p)$. Consequently, it must hold that $\nu \models p$.

Consider now the other direction where for some state ν it holds that $\nu \models p$. By definition of sat-atoms, its projection and S_1 we know that there must exist some $i^* \in \text{sat-atoms}(p) \downarrow_{J_p}$ such that $\nu \models i^*$. Moreover, there must exist an $o \in \text{sat-atoms}(p \wedge i^*)$ such that $\nu \models \bigwedge_{b \in o} b$. Finally, since $\nu \models i^* \wedge o$, there must exist an $A^* \in \text{sat-atoms}(p \wedge i^* \wedge o)$ such that $\nu \models \bigwedge_{a^* \in A^*} a^*$. Consequently, there exists a $(q_l, q_n) \in Q$ such that $\nu \models q_l \wedge q_n$ and therefore $\nu \models \bigvee_{(q_l, q_n) \in Q} q_l \wedge q_n$. \square

Proof of 10. Assume there were two linear queries $(i_1 \wedge \bigvee_j o_{1,j})$ and $(i_2 \wedge \bigvee_j o_{2,j})$ such that $i_1 \wedge i_2$ had a model. By definition, each set $A \in \text{sat-atoms}(p)$ must contain each atom of p or its negation. Consider now the projection $\text{sat-atoms}(p) \downarrow_{J_p}$ from which we obtain all i s (in particular i_1 and i_2): Since i_1 and i_2 contain the same set of atoms, it must be the case that for some atom $a \in i_1$, it holds that $\neg a \in i_2$ or vice versa (otherwise, the two would be identical). Through the law of the excluded middle, we get that $a \wedge \neg a$ is unsatisfiable, and thus $i_1 \wedge i_2$ is unsatisfiable. \square

Proof of 12. Assume some (ι, ω) is indeed a counterexample region for $q_l \wedge q_n$. In this case, we know that there is some $z \in \iota$ such that with $x^+ = g(z)$ we get $q_l(z, x^+) \wedge q_n(z, x^+)$. However, by definition of counterexample regions we also know that $g(z) = \omega(z)$. Therefore, the assignments of z and x^+ satisfy η . Next, consider the other direction. I.e. we assume we have a satisfying assignment

for η . By definition we know that for the given assignment of z it holds that $x^+ = g(z) = \omega(z)$. Therefore, z, x^+ respect the neural network and satisfy $q_l \wedge q_n$, which are the two requirements for a counterexample. \square

D Adaptive Cruise Control

Information on the $d\mathcal{L}$ model. The controller α_{ctrl} has three nondeterministic options: it can brake with $-B$ (no constraints), set relative acceleration to $a_{\text{rel}} = 0$ (constraint accCtrl_0) or choose any value in the range $[-B, A]$ (constraint accCtrl_1). The constraints for the second and third action are as follows:

$$\begin{aligned} \text{accCtrl}_0 &\equiv (2B(p_{\text{rel}} + Tv_{\text{rel}}) > v_{\text{rel}}^2) \\ \text{accCtrl}_1 &\equiv 2B(p_{\text{rel}} + Tv_{\text{rel}} + 0.5T^2a_{\text{rel}}) > (v_{\text{rel}} + Ta_{\text{rel}})^2 \wedge \\ &\quad (-v_{\text{rel}} > Ta_{\text{rel}} \vee 0 < v_{\text{rel}} \vee (v_{\text{rel}}^2 < 2a_{\text{rel}}p_{\text{rel}})) \end{aligned}$$

We can prove the safety of this control envelope for the following initial condition which is also the loop invariant:

$$\text{accInit} \equiv \text{accInv} \equiv p_{\text{rel}} > 0 \wedge p_{\text{rel}}2B \geq v_{\text{rel}}^2$$

The right-hand side of the invariant/initial condition ensures that the distance is still large enough to avoid a collision through an emergency brake ($a_{\text{rel}} = -B$). Based on these foundations, the full specification for the NN generated by VerSAILLE reads as follows:

$$\begin{aligned} &\left(0 \leq p_{\text{rel}} \wedge p_{\text{rel}} \leq 100 \wedge -200 \leq v_{\text{rel}} \wedge v_{\text{rel}} \leq 200 \wedge \right. \\ &\quad \left. -B \leq a_{\text{rel}}^+ \wedge a_{\text{rel}}^+ \leq A \wedge \right. \\ &\quad \left. p_{\text{rel}} > 0 \wedge p_{\text{rel}} \geq v_{\text{rel}}^2 / (2 * B) \right) \rightarrow \\ &\left(0 \leq T \wedge \text{cpost} = 0 \wedge a_{\text{rel}}^+ \geq A \wedge p_{\text{rel}}^+ = p_{\text{rel}} \wedge v_{\text{rel}}^+ = v_{\text{rel}} \vee \right. \\ &\quad \left. a_{\text{rel}}^+ \geq -B \wedge a_{\text{rel}}^+ < A \wedge a_{\text{rel}}^+ \neq 0 \wedge \right. \\ &\quad \left. ((-v_{\text{rel}}/a_{\text{rel}}^+ > T \vee -v_{\text{rel}} < 0) \wedge \right. \\ &\quad \left. p_{\text{rel}} + v_{\text{rel}} * T + a_{\text{rel}}^+ * T^2 / 2 > (v_{\text{rel}} + a_{\text{rel}}^+ * T)^2 / (2 * B) \vee \right. \\ &\quad \left. p_{\text{rel}} + v_{\text{rel}} * T + a_{\text{rel}}^+ * T^2 / 2 > (v_{\text{rel}} + a_{\text{rel}}^+ * T)^2 / (2 * B) \wedge \right. \\ &\quad \left. p_{\text{rel}} * a_{\text{rel}}^+ - v_{\text{rel}}^2 + v_{\text{rel}}^2 / 2 > 0) \wedge \right. \\ &\quad \left. 0 \leq T \wedge \text{cpost} = 0 \wedge p_{\text{rel}}^+ = p_{\text{rel}} \wedge rVel\text{post} = v_{\text{rel}} \vee \right. \\ &\quad \left. p_{\text{rel}} + v_{\text{rel}} * T > v_{\text{rel}}^2 / (2 * B) \wedge \right. \\ &\quad \left. 0 \leq T \wedge \text{cpost} = 0 \wedge a_{\text{rel}}^+ = 0 \wedge p_{\text{rel}}^+ = p_{\text{rel}} \wedge rVel\text{post} = v_{\text{rel}} \right) \end{aligned}$$

E Extended Evaluation

We implemented our procedure in a new tool⁶ called N³V. Due to the widespread use of ReLU NNs, N³V focuses on the verification of generic open-loop NNV queries for such NNs, but could be extended in future work. Our tool is implemented in Julia [15] using nnum [9, 11] for open-loop NNV, PicoSAT [16, 18] and Z3 [30, 50]. Our evaluation aimed at answering the following questions:

- Q1 Can N³V verify infinite-time horizon safety or exhaustively enumerate counterexample regions for a given NNCS?
- Q2 Does our approach advance the State-of-the-Art?
- Q3 Does our approach scale to complex real-world scenarios such as ACAS X?

⁶See <https://github.com/samysweb/NCubeV>

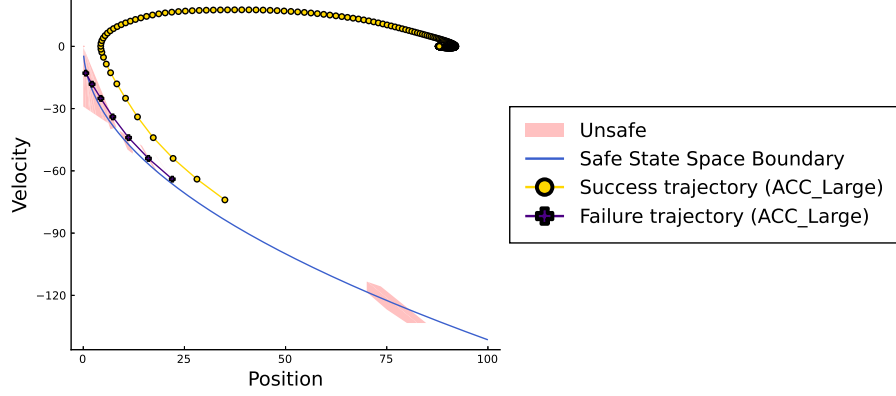


Figure 5: This plot shows the (input) state space for the ACC_Large NNCS: The blue line represents the boundary of the safe state space; the red areas indicate regions with counterexamples; the indigo and yellow line show potential trajectories of the system (dots represent discrete controller decisions).

The case studies comprised continuous and discrete control outputs. (Q3) is answered in the paper’s main evaluation (see Section 5; the remaining questions are discussed below. Times are wall-clock times on a 16 core AMD Ryzen 7 PRO 5850U CPU (N^3V itself is sequential while nenum uses multithreading).

E.1 Verification of Adaptive Cruise Control

We applied our approach to the previously outlined running example. To this end, we trained two NNs using PPO [79]: ACC contains 2 layers with 64 ReLU nodes each while ACC_Large contains 4 layers with 64 ReLU nodes each. Our approach only analyzes the hybrid system *once* and reuses the formulas for all future verification tasks (e.g. after retraining). We analyzed both NNs and a third one (see below for details) using N^3V for coarser and tighter approximation settings (using OVERT’s setting $N \in \{1, 2, 3\}$) on the value range $(p_{rel}, v_{rel}) \in [0, 100] \times [-200, 200]$. The analyses took 47 to 300 seconds depending on the NN and approximation. The runtimes show mixed results for tighter approximations: While tighter approximations (i.e. a higher N) sometimes improves performance (e.g. for ACC_Large retrained), it can also harm performance (e.g. as seen for ACC_Large). We suspect that this is a combination of two factors. First, finer approximations yield a larger number of queries which may increase the overall overhead. Secondly, our adjustments to OVERT’s approximation using approximation of piece-wise linearities (see Appendix B.1) may in some cases worsen the approximation in comparison to a lower N . We leave a more fine-grained analysis of approximation techniques to future work and focus our analysis on approximations with $N = 1$. Across all NNs we find that approximation helps: The first row shows performance when omitting the approximated constraints in the open-loop NN query and uniformly performs worse than an $N = 1$ approximation. N^3V finds the NN ACC_Large to be *unsafe* and provides an exhaustive characterization of all input space regions with unsafe actions.

Information on the counterexamples found for ACC_Large. Figure 5 shows the input state where the x-axis represents possible values for p_{rel} and the y-axis represents possible values for v_{rel} . The blue line represents the edge of the safe state space, i.e. all values below the blue line are outside the reachable state space of the contract. The red areas represent all parts of the state space where N^3V found concrete counterexamples for the checked controller monitor formula. Furthermore, the plot contains two lines representing the system’s evolution over time when started at certain initial states. In particular, we observe one trajectory leading to a crash due to an erroneous decision in the red area around $p_{rel} = 5, v_{rel} = -25$. This concrete counterexample was found by sampling initial states from the regions provided by N^3V .

Information on runtimes. The runtimes can be seen in Table 5 where #Filtered corresponds to the number of counterexample regions that were found to be spurious for ACC_Large. Comparing linear and $N = 1$ performance we see that approximation especially helps for larger NNs (ACC vs ACC_Large). This is the case because the overapproximate constraints can filter out numerous counterexample regions, which would otherwise have to be processed by the FILTER procedure. This

Approx.	ACC	ACC.Large	ACC.Large retrained	#Filtered
linear	65s	228s	277s	5658
$N = 1$	47s	87s	124s	1889
$N = 2$	53s	300s	70s	5604
$N = 3$	92s	139s	102s	1306

Table 5: Runtime of N^3V on the ACC networks per approximation. Final column lists filtered counterexamples for ACC.Large

Tool	Nonlinearities	Evaluated Configurations	Time (s)	Share of State Space	Result
NNV [88, 89, 92]	no	4	711	0.009%	safe for 0.1s
JuliaReach [17, 82]	no	4	—	0.009%	unknown
CORA [7]	yes	10	—	0.009%	unknown
POLAR [44]	poly. Zono.	12	—	0.009%	unknown
N^3V	polynomial	1	87	100.000%	safe for ∞

Table 6: Comparison of verification tools for NNCSs on the ACC Benchmark: Share of state space analyzed and best results of each tool.

effect is less significant for smaller networks where the time for overapproximation construction takes longer in comparison to the NN analysis time and less counterexamples are generated due to the lower number of ReLU nodes.

Further Training. Approx. 3% of ACC.Large’s inputs resulted in unsafe actions which demonstrably resulted in car crashes. We performed a second training round on ACC.Large where we initialized the system within the counterexample regions for a boosted $p \approx 13\%$ of all runs (choosing the best-performing p). By iterating this approach twice, we obtained an NN which was safe except for very small relative distances (for $(p_{rel}, v_{rel}) \in [0, 0.08] \times [-2, 0.1]$). N^3V certifies the safety outside this remaining region (see column ACC.Large retrained) which can be safeguarded using an emergency braking backup controller. Notably, this an *a priori* guarantee is for an arbitrarily long trip.

Results on Q1. Our tool N^3V is capable of verifying and refuting infinite-time horizon safety for a given $d\mathcal{L}$ contract. The support for exhaustively enumerating counterexamples can help in guiding the development of safer NNCSs.

E.2 Comparison to Other Techniques

Although Closed-loop NNV tools focus on finite-time horizons, we did compare our approach with the tools from ARCH Comp 2022 [64] on ACC. We began by evaluating safety certification on a small subset of the input space of ACC.Large (0.009% of the states verified by N^3V) for multiple configurations of each tool (see Table 6). Only NNV was capable of showing safety for 0.1 seconds (vs. time unbounded safety) while taking vastly longer for the tiny fraction of the state space.

Comparison to NNV. We performed a more extensive comparison to NNV by attempting to prove with NNV that the NNCS has no trajectories leading from within to outside the loop invariant. This would witness infinite-time safety. Due to a lack of support for nonlinear constraints, we approximate the regions. Over-approximating the invariant as an input region trivially produces unsafe trajectories, thus we can only under-approximate. Notably, this immediately upends any soundness or completeness guarantees (it does not consider all possible NN inputs nor all allowed actions). We apply an interval-based approximation scheme similar to OVERT (detailed in the subsequent paragraph). This scheme is parameterized by p_{rel} ’s step size (σ), v_{rel} ’s distance to the invariant (ϵ) and the step size for approximating the unsafe set (ρ). The right configuration of (σ, ϵ, ρ) is highly influential, but equally unclear. For example, with $\sigma = 0.25$, $\epsilon = 5$ and $\rho = 1$ we can “verify” not only the retrained ACC.Large NN for $2 \leq p_{rel} \leq 3$, but also the original, unsafe ACC.Large *despite concrete counterexamples*. This is a consequence of a coarse approximation, but also a symptom of a larger problem: Neither over- nor under-approximation yields useful results. In particular, discarding inputs close to the invariant’s edge equally removes states most prone to unsafe behavior (see Figure 5 in Appendix E.1).

Property	# Conjunctions	# Queries	# Feasible Conjunctions	# SMT calls
ACC	2.4k	20	86	261
ACC (Fallback)	5.1k	15	72	235
ACAS (DNC)	117.5M	1.7k	9.9k	11.4k
ACAS (DND)	88.9M	1.8k	10.4k	12.0k
ACAS (DES1500)	451.3B	12.5k	58.8k	66.4k
ACAS (CLI1500)	374.4B	13.1k	62.5k	70.4k
ACAS (SDES1500)	9.1T	18.6k	64.1k	75.8k
ACAS (SCLI1500)	18.2T	21.8k	76.0k	88.5k
ACAS (SDES2500)	39.0T	19.0k	66.7k	78.5k
ACAS (SCLI2500)	19.4T	18.6k	67.7k	79.8k

Table 7: Comparison of feasible conjunctions/queries for non-normalized open-loop NNV queries for an approximation with $N = 1$: #Conjunctions is the number of propositionally satisfiable conjunctions over linear constraints, # **Queries is the number of open-loop NNV queries generated by N^3V** , # Feasible Conjunctions is the number of open-loop NNV queries when splitting up disjunctions, # SMT calls is the number of feasibility checks performed by N^3V 's MOSAIC implementation during query generation.

Approximation Scheme employed for NNV. We consider input space stripes of width $\sigma > 0$, i.e. $(p_{rel}, v_{rel}) \in [p_0, p_0 + \sigma] \times [-\sqrt{2Ap_{rel}} + \epsilon, \frac{TB}{2}]$ (v_{rel} is bounded through the minimally allowed velocity and the maximal velocity that can still decrease p_{rel}). While σ determines the granularity of the under-approximation of NN inputs, $\epsilon > 0$ discards velocities too close to the loop invariant which cannot be proven using an underapproximation and must be non-zero to prove any system. For each stripe we compute the smallest reachable position p^* and compute a piece-wise linear overapproximation of the negated loop invariant $p_{rel} < v_{rel}^2 / (2A)$ on the interval $[p^*, p_0]$ using an approach conceptually similar to OVERT [85]. We determine the number of pieces through a step size $\rho > 0$, i.e. the interval $[p^*, p^* + \rho]$ will have a different line segment than the interval $[p^* + \rho, p^* + 2\rho]$. As the negation of the loop invariant (the blue line in Figure 5) is non-convex, we integrated an iterative check for disjunctions of unsafe sets into the verification procedure of NNV.

Comparison with DNNV (Table 7) As DNNV [84] does not support nonlinear properties, a direct comparison to the tool is impossible. However, we improve upon one important feature implemented in DNNV, namely query normalization. By exporting the boolean skeleton generated by MOSAIC, we can use projected model counting [83] to estimate the number of propositionally satisfiable conjunctions over linear constraints. Although the rule based normalization performed by DNNV may produce fewer formulas (this depends on the formula structure and implementation details of the rewriting system), this count provides an upper bound on the number of conjunctions that can be generated for a formula. Without MOSAIC, a rewriting system would first generate a large disjunctive normal form (with at most #Conjunction many elements), then check the feasibility of generated conjunctions and hand feasible conjunctions to an open-loop NNV tool. As indicated by Table 7, such an approach can lead to the number of conjunctions reaching into the trillions which becomes entirely intractable in practice. As can be seen in Table 7, our tool (# Queries) only produces a fraction of the propositionally satisfiable conjunctions (# Conjunctions) and also significantly reduces the number of open-loop NNV queries in comparison to an approach that splits up disjunctions (# Feasible Conjunctions). Note, that DNNV is also required to check generated conjunctions for feasibility, thus, our approach is also efficient in this regard by requiring a comparatively low number of SMT calls. Given the feasibility of 39 trillion conjunctions, one may wonder whether the propositional structure encoded in the boolean skeleton is of use at all. In this instance, we consider conjunctions over 110 distinct atoms. Indeed, the propositional structure adds value: Without it, we would obtain $2^{110} \approx 10^{33}$ possible conjunctions, i.e. based on the propositional structure we only consider a fraction of approx. 10^{-19} of all possible combinations. MOSAIC further reduces this fraction to a degree that is manageable via open-loop NNV.

Comparison with SMT solvers (Table 8) An alternative approach for the verification of non-linear open-loop NNV queries could be encoding the problem using an off-the-shelf SMT solver. In this case, the SMT solver has to check the satisfiability of the nonlinear Formula (9). We can instrument the Lantern package [40] to encode the NN into a SMT formula. Thus, we performed a comparison

Tool	ACC_Large		ACC_Large retrained	
	Status	Time	Status	Time
Mathematica	MO	—	MO	—
dReal	TO	—	TO	—
Z3	unknown	510s	unknown	1793s
Z3++	unknown	2550s	unknown	2269s
cvc5	TO	—	TO	—
MathSAT	TO	—	TO	—
N ³ V	sat	87s	unsat	124s

Table 8: Comparison of N³V with State-of-the-Art SMT solvers: Timeout (TO) was set to 12 hours

on the ACC_Large NN as well as the retrained ACC_Large NN, i.e. on a satisfiable as well as a non-satisfiable instance. We compared our approach to dReal [39], Mathematica [91], Z3 [30], MathSAT [25] (due to its use of incremental linearization) as well as the first and second place of SMT-Comp 2023 in the QF_NRA track: Z3++ [22] and cvc5 [13]. The results of our comparison can be observed in Table 8. The observed timeouts after 12 hours are unsurprising insofar as the work on linear open-loop NNV techniques was partially motivated by the observation that classical SMT solvers struggle with the verification of NNs.

Comparison to the techniques by Genin et al. [40] While the work by Genin et al. [40] represents a case-study with techniques specifically applied to an NN for a simplified airborne collision avoidance setting, some ideas from the example in [40] might in principle generalize to other case studies. Unfortunately, the case-study considered by [40] are not the NNs from Julian et al. [51, 53], but simplified NNs with a single acceleration control output. As the authors did not publish their trained NNs, their exact verification formulas, or their verification runtimes, we instead compare our approach with this line of work on our ACC benchmark. To this end, we approximate the verification property derived in Appendix E.1 using the box approximation techniques described by the authors and use their Lantern Python package to translate the verification tasks into linear arithmetic SMT problems. Using Z3, their technique does not terminate within more than 50 hours on the (unsafe) ACC_Large network and thus fails to analyze the NN. This demonstrates significant scalability limitations compared to our approach. Moreover, it is worth pointing out that the authors themselves acknowledge that the technique is incomplete which distinguishes our complete lifting procedure from their approach.

Results on Q2. If closed-loop NNV is a hammer then guaranteeing infinite-time safety is a screw: It is a categorically different problem requiring a different tool. N³V provides safety guarantees which go infinitely beyond the guarantees achievable with State-of-the-Art techniques (closed-loop NNV or otherwise). A direct CAD/SMT encoding of Formula (9) as well as the techniques by Genin et al. [40] are no alternatives due to timeouts (>12h) or “unknown” results (see also Table 8).

E.3 Zeppelin Steering

As a further case study, we considered the task of steering a Zeppelin under uncertainty: The model’s goal was to learn avoiding obstacles while flying in a wind field with nondeterministic wind turbulences. This problem has previously been studied with differential hybrid games [74]. The examined scenario serves two purposes: On the one hand, it shows that our approach can reuse safety results from the $d\mathcal{L}$ literature which drastically increases its applicability; on the other hand it is a good illustration for why verification (rather than empirical evidence) is so important when deploying NNs in safety-critical fields.

After transferring the differential hybrid games logic contract into a differential dynamic logic contract and proving its safety, we trained a model to avoid obstacles while flying in a wind field with uniformly random turbulences via PPO. After 1.4 million training steps, we obtained an agent that did not crash for an evaluation run of 30,000 time steps. Given these promising results we proceeded to verify the agent’s policy assuming a safe – or at least “almost safe” – flight strategy had been learnt. However, upon verifying the NN’s behavior for obstacles of circumference 40, we found that it produced potentially unsafe actions for large parts of the input space. The reason this unsafety was

not observable during empirical evaluation was the choice of uniformly random wind turbulences: The unsafe behavior only appears for specific sequences of turbulences which occur extremely rarely in the empirical setting. This flaw in the training methodology was only found due to the verification. This is where our approach differs from simulation-based evaluation: With an SMT filter timeout of 4 seconds, N^3V provides an *exhaustive* characterization of *all* potentially unsafe regions in 4.1 hours while providing 72 concrete counterexample regions. This is where our approach differs from simulation-based evaluation, as we were able to generate an exhaustive characterization of counterexample regions. In this instance, the tool’s bottlenecks were approximation construction and the SMT based counterexample finding. This case study and the stark difference between simulation and verification underscore the importance of rigorous verification of NNs as an addition to empirical evidence in safety-critical areas.

F Allowed advisories for Vertical Airborne Collision Avoidance

Table 9 provides an overview of possible advisories for a Vertical Airborne Collision Avoidance System. The allowed range of vertical velocity and the required minimal acceleration are integrated into the $d\mathcal{L}$ model used by VerSAILLE.

Advisory	Description	Vertical Velocity [ft/min]	Min. Acceleration
COC	Clear of conflict	—	—
DNC	Do not climb	$[-\infty, 0]$	$g/4$
DND	Do not descend	$[0, \infty]$	$g/4$
DES1500	Descend at least 1500 ft/min	$[-\infty, -1500]$	$g/4$
CL1500	Climb at least 1500 ft/min	$[1500, \infty]$	$g/4$
SDES1500	Strengthen descent to at least 1500 ft/min	$[-\infty, -1500]$	$g/3$
SCL1500	Strengthen climb to at least 1500 ft/min	$[1500, \infty]$	$g/3$
SDES2500	Strengthen descent to at least 2500 ft/min	$[-\infty, -2500]$	$g/3$
SCL2500	Strengthen climb to at least 2500 ft/min	$[2500, \infty]$	$g/3$

Table 9: Overview on Vertical Airborne Collision Advisories (simplified version of [48, Table 1])

G NMACs produced by NN-based ACAS X advisories

Further counterexamples for the advisories of the NNCS can be found in Figures 6 to 10.

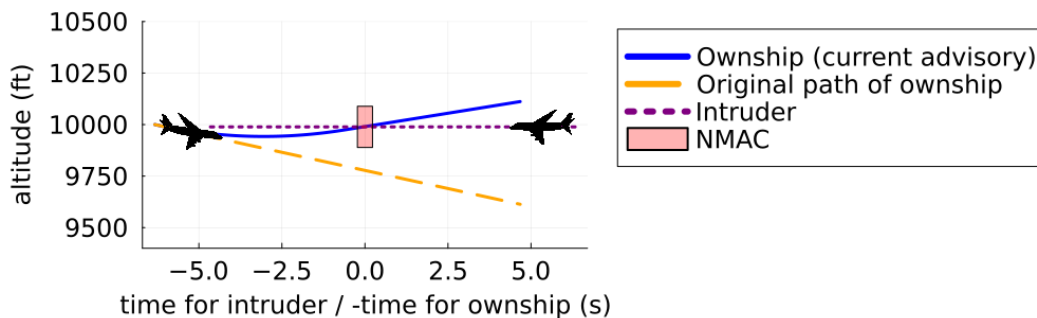


Figure 6: After a previous advisory to descend at least 1500ft/min, the NN advises the pilot to strengthen climb to at least 1500ft/min leading to a NMAC.

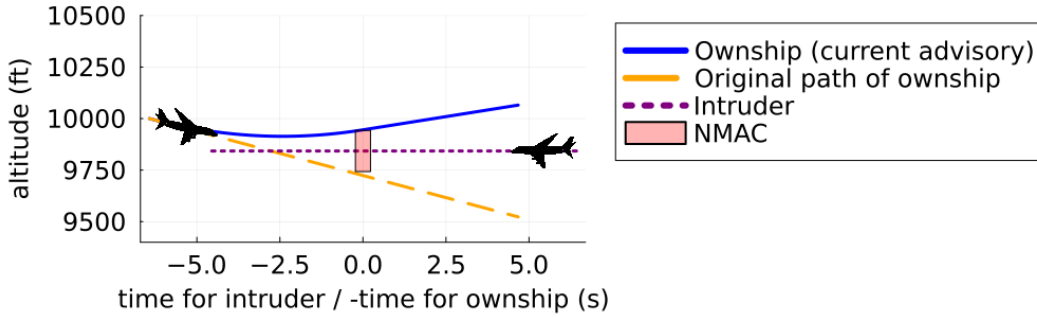


Figure 7: After a previous advisory to strengthen descent to at least 1500ft/min, the NN advises the pilot to strengthen climb to at least 1500ft/min leading to a NMAC.

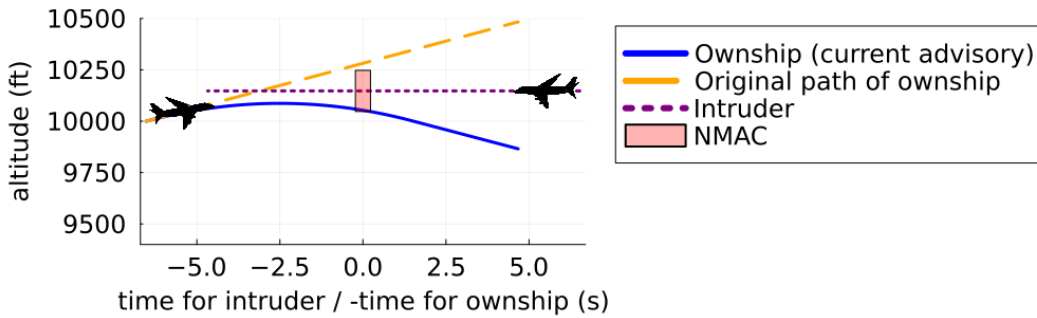


Figure 8: After a previous advisory to strengthen climb to at least 1500ft/min, the NN advises the pilot to strengthen descent to at least 2500ft/min leading to a NMAC.

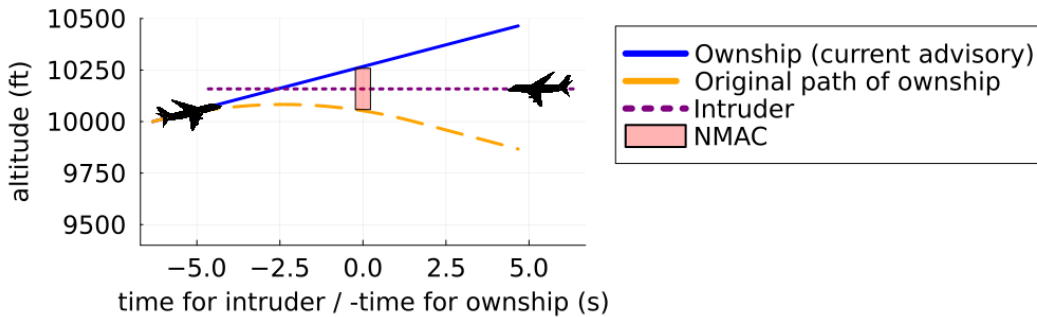


Figure 9: After a previous advisory to strengthen descent to at least 2500ft/min, the NN advises the pilot to strengthen descent to at least 2500ft/min leading to a NMAC.

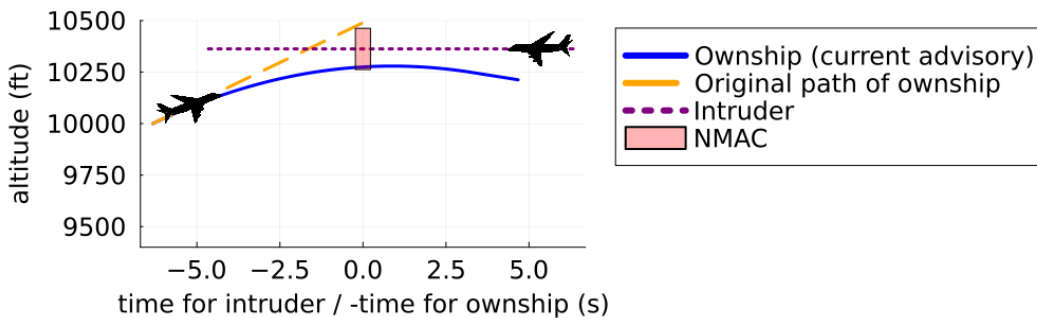


Figure 10: After a previous advisory to strengthen climb to at least 2500ft/min, the NN advises the pilot to strengthen descent to at least 1500ft/min leading to a NMAC.

Counterexamples to the safety of NNCS advisories for non-level flight of the intruder in the case of a previous advisory *Do Not Climb* and *Do Not Descend* can be found in Figures 11 and 12. Note, that for non-level flight (i.e. both intruder and ownship have a non-zero vertical velocity), there exist two possible interpretations for the advised vertical velocities. These can be interpreted as absolute or relative velocity. For our counterexamples in Figures 11 and 12 we opt for the relative velocity interpretation. This does not affect the analysis for level flight intruders where the interpretations coincide.

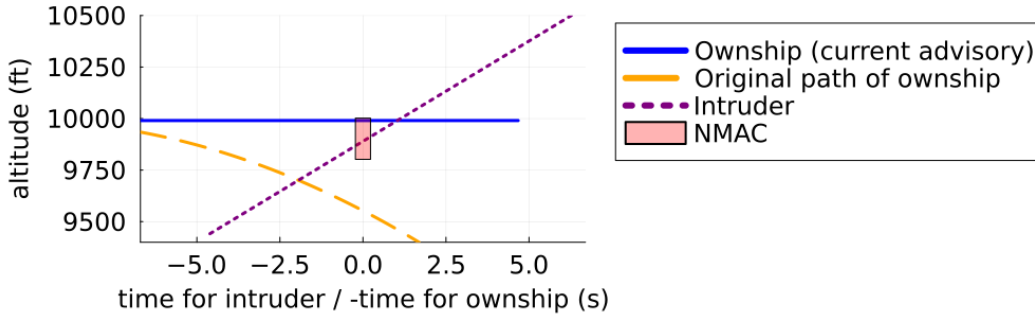


Figure 11: After a previous advisory to not climb, the NN advises the pilot to climb with at least 1500ft/min leading to a NMAC.

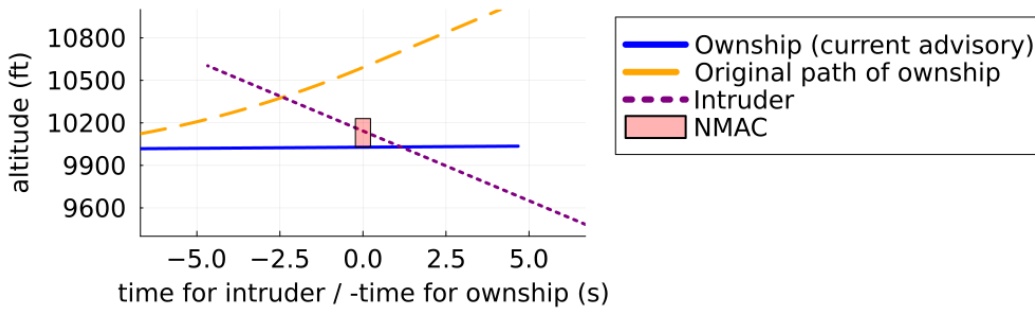


Figure 12: After a previous advisory to not descend, the NN advises the pilot to descend with at least 1500ft/min leading to a NMAC.